A SENSITIVITY STUDY OF THE CRITICAL FLOW MODELS USED IN RELAP4/MOD5 BLOWDOWN ANALYSIS OF A GENERAL ELECTRIC BWR.

Mark Vearil Carle

UNCLASS

SECURITY CLASSIFICATION OF THIS PAGE (When Data Entered)

REPORT DOCUMENTATION PAGE		READ INSTRUCTIONS BEFORE COMPLETING FORM
1. REPORT NUMBER	2. GOVT ACCESSION NO.	3. RECIPIENT'S CATALOG NUMBER
4. TITLE (and Subtitle) A SENSITIVITY STUDY OF THE CRITICAL FLOW MODELS USED IN RELAP4/MOD 5 BLOWDOWN ANALYSIS OF A GENERAL ELECTRIC BWR		5. TYPE OF REPORT & PERIOD COVERED THESIS 6. PERFORMING ORG. REPORT NUMBER
7. AUTHOR(s) CARLE, MARK V.		8. CONTRACT OR GRANT NUMBER(s)
9. PERFORMING ORGANIZATION NAME AND ADDRESS PENNSYLVANIA STATE UNIVERSITY		10. PROGRAM ELEMENT, PROJECT, TASK AREA & WORK UNIT NUMBERS
11. CONTROLLING OFFICE NAME AND ADDRESS CODE 031 NAVAL POSTGRADUATE SCHOOL MONTEREY, CALIFORNIA, 93940		12. REPORT DATE NOV 78 13. NUMBER OF PAGES 88
14. MONITORING AGENCY NAME & ADDRESS(if different from Controlling Office)		15. SECURITY CLASS. (of this report) UNCLASS 15a. DECLASSIFICATION/DOWNGRADING SCHEDULE

16. DISTRIBUTION STATEMENT (of this Report)

APPROVED FOR PUBLIC RELEASE; DISTRIBUTION UNLIMITED

17. DISTRIBUTION STATEMENT (of the abstract entered in Block 20, if different from Report)

18. SUPPLEMENTARY NOTES

19. KEY WORDS (Continue on reverse side if necessary and identify by block number)

GENERAL ELECTRIC BWR, RELAP 4/MOD 5, CRITICAL FLOW MODELS

20. ABSTRACT (Continue on reverse side if necessary and identify by block number)

SEE REVERSE.

DD FORM 1 JAN 73 1473 (Page 1)

EDITION OF 1 NOV 65 IS OBSOLETE

S/N 0102-014-6601 |

UNCLASS

SECURITY CLASSIFICATION OF THIS PAGE (When Data Entered)

ABSTRACT

This study utilizes the RELAP4/MOD5 Computer Code to analyze the effects of critical flow modeling on the thermal-hydraulic transient response of a General Electric boiling water reactor to a major primary coolant line rupture. Included in the study is a presentation of the equations, assumptions, and limitations of the critical flow models available for use in RELAP4. Additionally, an evaluation of a temporary solution to a RELAP4 coding error associated with stagnation properties calculation is presented.

The results of this investigation indicate that; (1) A solution to the stagnation properties calculational error that exists in the RELAP4 code, when applied to the Evaluation Model, (RELAP4-EM) provides a conservative evaluation, relative to the Standard Model (RELAP4-SM), regardless of which of the five critical flow models available in the code is selected; (2) Of the five critical flow models available for use in RELAP4, the Moody model and the Henry-Fauske model are nearly equivalent in their relative degrees of conservatism. Following these models, in order of relative degree of conservatism, are the Modified Momentum/Homogeneous Equilibrium model, the Homogeneous Equilibrium model, and the Sonic

model; (3) In order to best alleviate the stagnation properties coding error, the flow areas for the volumes immediately upstream from the recirculation line rupture should be increased such that the area ratio (break flow area / upstream volume flow area) is 0.7.

The Pennsylvania State University

The Graduate School

Department of Nuclear Engineering

A Sensitivity Study of the Critical Flow Models Used in RELAP4/MOD5 Blowdown Analysis of a General Electric BWR

A Masters of Engineering paper in

Nuclear Engineering

by

Mark Vearil Carle

Submitted in Partial Fulfillment
of the Requirements
for the Degree of

Masters of Engineering

November 1978

Date of Approval:

ABSTRACT

This study utilizes the RELAP4/MOD5 Computer Code to analyze the effects of critical flow modeling on the thermal-hydraulic transient response of a General Electric boiling water reactor to a major primary coolant line rupture. Included in the study is a presentation of the equations, assumptions, and limitations of the critical flow models available for use in RELAP4. Additionally, an evaluation of a temporary solution to a RELAP4 coding error associated with stagnation properties calculation is presented.

The results of this investigation indicate that; (1) A solution to the stagnation properties calculational error that exists in the RELAP4 code, when applied to the Evaluation Model, (RELAP4-EM) provides a conservative evaluation, relative to the Standard Model (RELAP4-SM), regardless of which of the five critical flow models available in the code is selected; (2) Of the five critical flow models available for use in RELAP4, the Moody model and the Henry-Fauske model are nearly equivalent in their relative degrees of conservatism. Following these models, in order of relative degree of conservatism, are the Modified Momentum/Homogeneous Equilibrium model, the Homogeneous Equilibrium model, and the Sonic

model; (3) In order to best alleviate the stagnation properties coding error, the flow areas for the volumes immediately upstream from the recirculation line rupture should be increased such that the area ratio (break flow area / upstream volume flow area) is 0.7.

TABLE OF CONTENTS

LIST OF TABLES

LIST OF FIGURES

NOMENCLATURE

a = sonic velocity

A = flow area

α = void fraction

β = coefficient of isobaric thermal expansion

C_P = specific heat capacity at constant pressure

C_V = specific heat capacity at constant volume

ΔP = differential or change in pressure

Δt = time step size

F = viscous forces

G = mass flow rate per unit area (mass flux)

g_c = gravitational constant

γ = ratio of specific heat capacities

h = enthalpy

I = junction inertia

J = mechanical equivalent of heat

K = coefficient of isothermal compressibility

M = lumped parameter accounting for friction and momentum changes

N = nonequilibrium parameter

n = polytropic process exponent

P = pressure

R = critical pressure/stagnation pressure ratio

ρ = density

S = slip ratio

s = entropy

σ = surface tension

V = velocity

v = specific volume

W = mass flow rate

X = quality

z = distance in direction of fluid travel

SUBSCRIPT NOTATION

b = downstream or back

C = critical

f = liquid

g = vapor

j = junction

SAT = saturated conditions

T = transition completion point

t = time at particular time step

$t+\Delta t$ = time at following time step

UP = upstream

o = stagnation

ACKNOWLEDGEMENTS

The author wishes to express his sincere appreciation to Dr. Gordon E. Robinson for his advice and encouragement during the preparation of this work; to Dr. Warren F. Witzig, Dr. Forrest J. Remick, and Dr. Gordon E. Robinson for their critical reviews of the writing; and to the United States Navy which provided the time and funds for the pursuit of this degree.

1. INTRODUCTION

1.1 GENERAL

The United States, in its fourth decade of nuclear reactor research and operation, now has seventy-two civilian power reactors in operation and has generated over a trillion megawatt-hours of electricity. Since the inception of the nuclear power industry, safety has been the major consideration in the design, construction, and operation of nuclear power plants.

Modern experimental programs in water-reactor safety are directed toward improving the ability to understand specific phenomena and the results of tests, with the goal of applying this understanding to the interpretation of "similar" phenomena that might take place if a reactor accident were to occur. Complex digital computer codes have been developed to predict the thermal-hydraulic transient response of nuclear reactor systems to hypothesized accidents. Verification of specific portions of these computer codes is the goal of an ongoing experimental water-reactor safety program.

1.2 LOSS-OF-COOLANT ACCIDENT (LOCA)

A LOCA is generally defined as any accident which causes the coolant to be lost from the cooling system serving the reactor core. The design-basis LOCA is that primary system pipe rupture which results in maximizing the fuel-rod cladding temperatures attained during the accident.

For boiling water reactors (BWRs) the design-basis LOCA is a double-ended guillotine break of one of the two coolant recirculation lines. The coolant recirculation lines are the primary means of maintaining coolant flow through the reactor core, and are the largest diameter piping in the primary system. Emergency core cooling systems (ECCS) are designed to provide cooling to the core in order to prevent fuel element melt down in the event of a design-basis LOCA. Future references to LOCA will imply design-basis LOCA unless otherwise indicated.

Within the present regulatory framework, the thermal-hydraulics of a LOCA can be described as having three distinct phases known as blowdown, refill, and reflood (2).
(1) Reactor Blowdown: During the reactor depressurization or blowdown phase, reduction of core flow and increase in the local quality result in departure from nucleate boiling (DNB) and dry-out of the core. Following the establishment of the conditions causing DNB, the heat transferred from the fuel rods to the coolant decreases markedly, and the

temperature of the fuel rods, and the fuel-rod cladding, rises rapidly. Depressurization continues until primary system and containment pressures are equalized and the break flow is essentially zero.

(2) Refill and Reflood: At the end of the blowdown phase, the liquid coolant inventory in the system is small, and the core may be completely immersed in steam. The system pressure is low, on the order of 50 to 100 PSIA. As the ECCS starts injecting emergency coolant, refilling of the lower plenum begins. For conservative safety evaluations, heat transfer to the coolant is often totally ignored during this refill phase. When the liquid level reaches the bottom of the core, the reflooding phase begins. As the liquid level rises in the core a tremendous amount of heat is removed from the fuel rods due to vaporization of the incoming liquid. Peak cladding temperatures will be attained during this phase of the accident.

For an excellent, detailed physical description of a BWR LOCA the interested reader is referred to references (3) and (4).

1.3 CODE DESCRIPTION

RELAP4 is a computer program, written in Fortran IV, that was developed primarily to describe the thermal-hydraulic transient behavior of water-cooled nuclear

reactors subjected to postulated accidents such as those resulting from loss of coolant, pump failure or nuclear power excursions. Fundamental assumptions inherent in the thermal-hydraulic equations used in the code are that a two-phase fluid is homogeneous and that the phases are in thermal equilibrium. Models are available to modify the homogeneous assumption.

The program is currently available in its fourth major revision, hence RELAP4. The edition of the program installed at The Pennsylvania State University is RELAP4/MOD5-UPDATE2 (henceforth referred to as RELAP4).

There are four major options available in RELAP4. The Evaluation Model option, hereafter referred to as RELAP4-EM, is intended to provide conservative results which meet most of the requirements for licencing under Appendix K to 10 CFR Part 50. Another option available, called the Standard Model (RELAP4-SM), is used to provide the best estimate of the actual expected response during a LOCA. While RELAP4 was primarily designed to be a blowdown code, it is capable of representing the LOCA transient through reflood in pressurized water reactors (RELAP4-FLOOD option). Also available is the containment option (RELAP4-CONTAINMENT), which can be used to evaluate the effectiveness of ice-condenser containment systems. The two main options that will be used in this study are RELAP4-EM and RELAP4-SM.

RELAP4 requires numerical input data which completely describes the initial conditions and the geometry of the system being analyzed. Included in the input data are physical characteristics such as fluid volume, geometry, pump characteristics, power generation, and material composition. Transients can be initiated by the control action inputs to the program. These controls can describe breaks in fluid piping, core power level variations including a SCRAM, valve actions, etc. For each time advancement the program computes fluid conditions such as flow, pressure, quality, and mass inventory. Also computed are thermal conditions within the solid materials such as temperature profiles and power generated, and the fluid-solid interface conditions such as heat flux and surface temperature.

A complete theoretical development of the code, as well as implementation procedures, is contained in the RELAP4/MOD5 Users Manual (5). An excellent description with specific reference to BWR LOCA analysis is also available in a masters thesis by Laird (3).

The reactor system used for this study is the Hope Creek Nuclear Power Generating Station. This General Electric BWR was modeled for RELAP4 by Idaho National Engineering Laboratory (INEL) personnel, and was included as a sample problem with the RELAP4 transmittal tape.

The thermal-hydraulic model of Hope Creek, depicted in Figure 1, consists of twenty-three control volumes, thirty-three junctions, and twenty-five heat slabs. Table 1, pages 8 and 9, presents a description of the twenty-three control volumes used in this model. Junctions simply connect control volumes, and heat slabs represent sections of the physical system which can absorb, radiate, store, or generate heat. RELAP4-EM and RELAP4-SM data input decks used in this study are discussed in Appendix A.

1.4 CRITICAL FLOW

"When a fluid expands from a compressed state to arbitrary ambient (or "receiver") conditions in passage through an outlet, the flow rate is always less than a certain maximum or "critical" value. After this critical condition has been reached, further reductions in receiver pressure leave the flow rate unaltered, serving only to form a steep pressure gradient at some location in the outlet passage (6)." This condition is commonly called critical, or choked, flow.

At the instant of recirculation line rupture the flow rate out of the break increases until critical flow conditions are reached. There are five critical flow models available in RELAP4 to predict this critical flow rate. They are, (1) The Sonic model, (2) The Moody model, (3) The

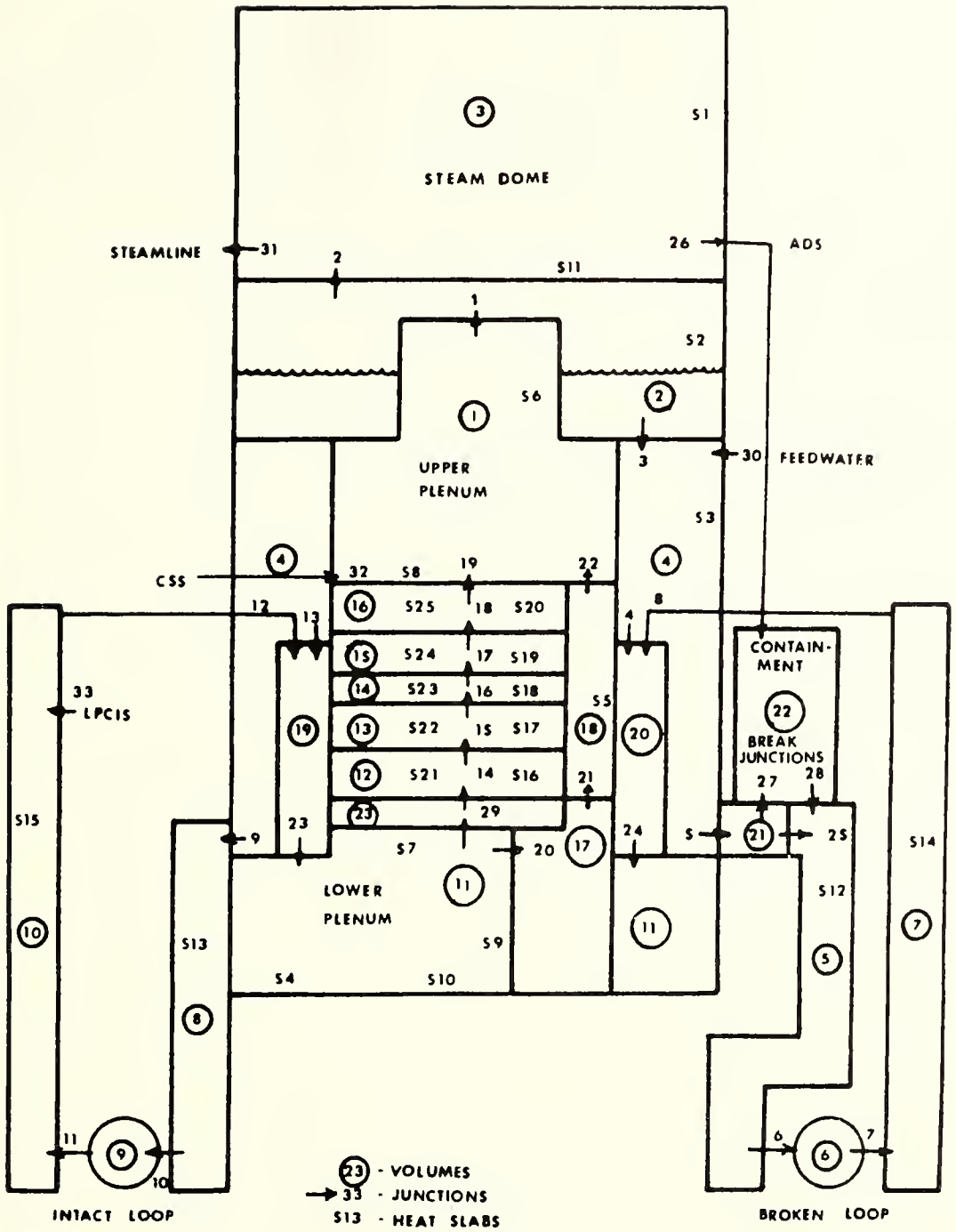

FIGURE 1
RELAP4 MODEL OF G. E. BWR

Table 1. Volume Descriptions in RELAP4 Model

Volume No.	Description
1	Upper Plenum and Steam Separators
2	Upper Downcomer (This volume extends from the feedwater entry point to the bottom of steam dryers.)
3	Steam Dome (This volume contains the high quality steam located above the dryers.)
4	Lower Downcomer (This volume contains the subcooled water which enters the downcomer from the feedwater entry point. The lower downcomer describes the region of the downcomer between the feedwater entry point and the entry point of the feedwater into the lower plenum.)
5	Broken Loop Recirculation Suction Line (This volume models the 26" pipe which pulls the saturated water from the lower downcomer into the jet pump of the broken loop. Although the break occurs along this suction line, the actual break volume is modeled by volume 21.)
6	Broken Loop Recirculation Pump
7	Broken Loop Recirculation Discharge Line (This volume models the 24" line which returns the water from the recirculation pump to the jet pump intake.)
8	Intact Loop Recirculation Suction Line
9	Intact Loop Recirculation Pump
10	Intact Loop Recirculation Discharge Line
11	Lower Plenum
12-16	Heated Core Sections (With the addition of volume 23, these volumes model the core. To achieve relatively equal thermodynamic characteristics, the heated core sections vary in height from 2.85 feet to 1.00 feet.)
17	Guide Tubes (The control rod guide tubes in the lower plenum and the unheated segment of the core are modeled as one control volume.)

Table 1. (cont.)

Volume No.	Description
18	Core Bypass (This volume represents the region between the fuel assemblies in the core.)
19	Intact Loop Jet Pump (This volume models the intact loop jet pumps from the intake to the exhaust into the lower downcomer. Each bank of ten jet pumps is modeled as one volume.)
20	Broken Loop Jet Pump (This single volume models the bank of ten jet pumps in the broken loop.)
21	Break Volume (This volume is specified between the broken loop recirculation discharge line and the lower downcomer.)
22	Containment
23	Unheated Segment of the Core

Henry-Fauske model, (4) The Homogeneous Equilibrium model, and, (5) The Modified Momentum/Homogeneous Equilibrium model. These models are discussed in detail in Chapter Two of this study.

The simple momentum equation for inertial flow rate is quite accurate at low flow rates but becomes greatly exaggerated as the driving pressure differential increases and critical conditions are approached. RELAP4 computes the flow rate using the simple momentum equation and compares this flow rate to that predicted by the selected critical flow model. The minimum is then selected as depicted by the solid line in Figure 2 (7).

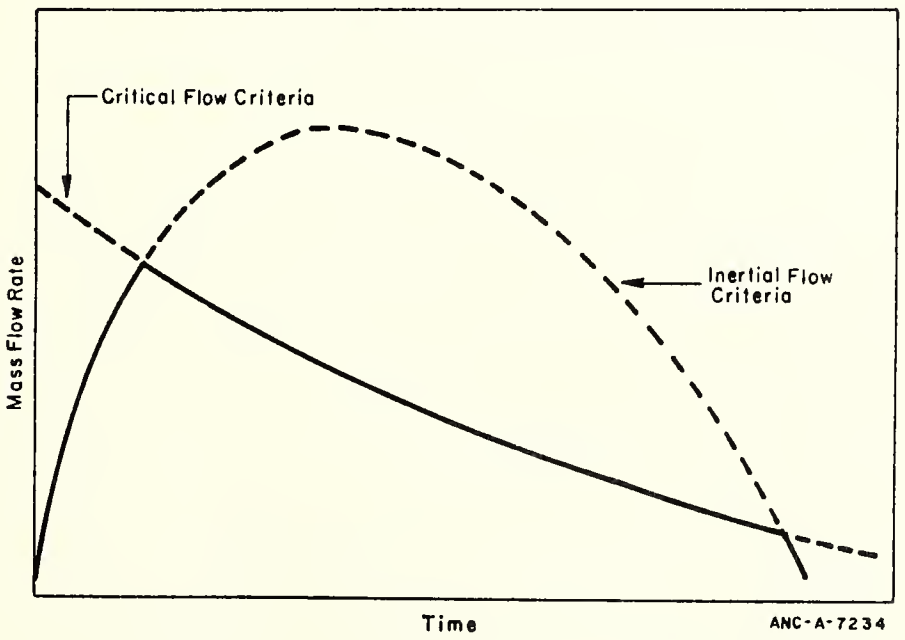

FIGURE 2
JUNCTION MASS FLOW RATE SELECTION

1.5 STAGNATION PROPERTIES

All of the critical flow models available in RELAP4, with the exception of the Sonic model, require that stagnation properties be calculated for the volume upstream of the junction undergoing critical flow. These calculations are performed by a subroutine called STAGP.

The stagnation pressure and enthalpy are calculated from the static pressure and enthalpy using a calculated fluid velocity. An isentropic path from the static to the stagnation enthalpy-pressure point is followed.

The stagnation enthalpy is calculated from the kinetic energy relationship:

$$h_o = h_l + V^2/2g_cJ \qquad (1)$$

where V is calculated from the following relationship:

$$V = Wv/A \quad . \qquad (2)$$

The quantities h_l, W, and v are evaluated at the junction, A is the upstream volume flow area.

In equation (1), V is not allowed to be greater than the isentropic sonic velocity of the upstream volume.

Applying the first law of thermodynamics in differential form for a fluid undergoing a flow change provides, (Gibbs equation);

$$Tds = dh - vdP \quad . \tag{3}$$

For an isentropic process, ds = 0. Then,

$$dP = dh/v \quad . \tag{4}$$

Integrating this for the change in enthalpy and applying static and stagnation limits provides:

$$P_o = P_1 + \int_{h_1}^{h_o} dh/v \tag{5}$$

where v, the specific volume, is a function of P and h, and P_o and P_1 are the stagnation and static pressures, respectively.

Equation (5) is advanced from (h_1,P_1) to (h_o,P_o) by a fourth-order Runge-Kutta subroutine.

It had been reported that there existed a logic problem in the stagnation properties subroutine, STAGP, requiring the elimination of this routine from the RELAP4 logic (8, 9). It has since been discovered, and disclosed at the INEL Code Users Workshop conducted at INEL, Idaho Falls, Idaho 8/28/78 thru 9/1/78, that the stagnation properties calculation problem was not due to a logic error in the STAGP subroutine, but rather was due to the fact that the code was predicting velocities greater than the isentropic sonic velocity for the volume immediately upstream of the break junction.

As pointed out earlier, the code does not allow the calculated velocity in equation (1) to exceed the isentropic sonic velocity of the upstream volume. If the junction conditions are such that equation (2) predicts a velocity greater than sonic, erroneous values for the stagnation pressure and enthalpy will result.

The "fix" suggested at the workshop was to artificially increase the upstream volume flow area (the denominator of equation (2)) in order to prevent supersonic velocity predictions from occurring. This flow area increase should be carried out for all volumes where critical flow is likely to occur.

1.6 PURPOSE

The purpose of this study is threefold;

(1) Review the derivation of the equations for each of the critical flow model options available in RELAP4.

(2) Determine by what amount the upstream volume flow area must be increased in order to alleviate the problem in calculating stagnation properties that was reported in the previous section.

(3) Present a sensitivity study on the critical flow models available in RELAP4 and rate the models as to their relative degrees of conservatism.

2. CRITICAL FLOW MODELS

2.1 INTRODUCTION

As previously reported, there are five critical flow models available in RELAP4. They are:

(1) The Sonic model (10),

(2) The Moody model (11),

(3) The Henry-Fauske model (12),

(4) The Homogeneous Equilibrium model (13), and

(5) The Modified Momentum/Homogeneous Equilibrium model (14).

For each junction in the system the user must specify whether the code is to use one of these models or the simple momentum (inertial flow) equations to estimate the flow rate through that junction. In addition the user may select from eighteen possible combinations of these models. For example the user may elect to use the Sonic model when the fluid is subcooled and the Moody model when the fluid is saturated. These combinations, as well as the selection methods, are discussed in the RELAP4/MOD5 Users Manual (15).

The purpose of this chapter is to present each of the critical flow models listed above, providing the basic assumptions and limitations of each. In addition, at the end of this chapter a brief description of the logic involved in junction flow rate estimation is given.

2.2 THE SONIC MODEL (10)

As the name implies, this model assumes that the junction flow rate is that which will result in sonic velocity at the junction.

The sonic velocity of the fluid is calculated from,

$$a^2 = [Xv_g+(1-X)v_f]^2 g_c T(P')^2/\{X[C_{p_g} J+TP'v_g(P'K_g-2\beta_g)] + (1-X)[C_{p_f} J + TP'v_f(P'K_f - 2\beta_f)]\} \quad (6)$$

where P' signifies the derivative of the partial pressure with respect to temperature.

It is important to note that the independent variables in equation (6) are based upon the upstream volume conditions. That is, the steam tables are entered with upstream volume specific internal energy and specific volume as the independent variables. All other upstream volume parameters, including pressure and sonic velocity, are dependent on these two quantities. The result is that the upstream volume critical velocity is calculated and then impressed upon the local downstream junction.

The critical mass flow rate through the junction is calculated from the one-dimensional continuity equation,

$$W = \rho A_j a \quad . \quad (7)$$

The density used in equation (7) is calculated from the upstream volume density as follows. The upstream volume density is first adjusted for the frictional loss and kinetic energy changes to the junction. The fluid is then expanded isentropically from the Mach number just upstream from the junction to that in the junction, which is Mach one, when sonically choked. It should be noted that A_j is the flow area at the junction.

The assumptions implicit in the use of this model are:

(1) The critical flow rate is assumed to be that which will result in sonic velocity at the junction,

(2) The critical flow rate is given by the one-dimensional continuity equation,

(3) The junction critical velocity is based upon upstream volume fluid conditions, and

(4) In calculating the density used in equation (7) isentropic expansion is assumed.

This model is also capable of predicting critical flow rates when the upstream volume contains air or a mixture of air and saturated or superheated steam. This capability is relevant only to the containment option (RELAP4-CONTAINMENT) and will not be further discussed.

2.3 THE MOODY MODEL (11)

The Moody model is applicable only in the saturated region, and therefore is used primarily in low pressure systems. It is the only critical flow model available in RELAP4 which allows for slip between phases. In addition it does not rely on empirical data for its derivation.

The derivation of the equation for critical mass flux starts with the continuity and energy equations for two-phase, annular flow;

$$G = W/A = \alpha V_g/Xv_g = (1 - \alpha)V_f/(1 - X)v_f \qquad (8)$$

$$h_o = X(h_g + V_g^2/2g_cJ) + (1 - X)(h_f + V_f^2/2g_cJ) \quad . \qquad (9)$$

X and α are defined by,

$$X = W_g/W \quad ; \quad 1 - X = W_f/W \qquad (10)$$

$$\alpha = A_g/A \quad ; \quad 1 - \alpha = A_f/A \quad . \qquad (11)$$

The ratio of average vapor velocity to average liquid velocity is the slip ratio, S ;

$$S = V_g/V_f \quad . \qquad (12)$$

Rewriting equation (8) and substituting equation (12) yields,

$$V_g/V_f = (1 - \alpha)Xv_g/\alpha(1 - X)v_f = S \quad . \tag{13}$$

Solving for the void fraction in terms of the slip ratio yields,

$$\alpha = 1/\{1 + [Sv_f(1 - X)/Xv_g]\} \quad . \tag{14}$$

Assuming that the expansion is isentropic ($s = s_o$), and from the definition of quality,

$$X = (s_o - s_f)/s_{fg} \tag{15}$$

or

$$1 - X = (s_g - s_o)/s_{fg} \quad . \tag{16}$$

An expression for the mass flux G is obtained by combining equations (8) through (16) as follows;

Rewriting equation (9) yields,

$$2g_c J[h_o - h_f - X(h_g - h_f)] = V_g^2[X + V_f^2(1-X)/V_g^2] \tag{17}$$

Substituting equation (12) into equation (17) and noting that $h_{fg} = h_g - h_f$ yields,

$$2g_c J[h_o - h_f - Xh_{fg}] = V_g^2[X + (1 - X)/S^2] \quad . \tag{18}$$

Rewriting equation (14) as,

$$\alpha = Xv_g/[Xv_g + Sv_f(1 - X)] \quad , \tag{19}$$

solving equation (8) for V_g, and substituting equation (19) yields,

$$V_g = G[Xv_g + Sv_f(1 - X)] \quad . \tag{20}$$

Substituting equation (20) into equation (18) and solving for G yields,

$$G^2 = 2g_c J(h_o - h_f - Xh_{fg})/ \{[Xv_g + Sv_f(1 - X)]^2[X + (1 - X)/S^2]\} \quad . \tag{21}$$

Substituting equations (15) and (16) into equation (21) yields,

$$G^2 = 2g_c J[h_o - h_f - h_{fg}(s_o - s_f)/s_{fg}]/$$

$$\{[Sv_f(s_g - s_o)/s_{fg} + v_g(s_o - s_f)/s_{fg}]^2 \qquad (22)$$

$$[(s_o - s_f)/s_{fg} + (s_g - s_o)/S^2 s_{fg}]\} \quad .$$

Note from equation (22) that if h_o and s_o are known, then G is a function of S and P (ie. knowing the pressure and the fact that saturation exists fixes all of the quantities in equation (22) except h_o, s_o, and S).

Therefore, if G has a maximum it must satisfy the necessary conditions,

$$\left.\frac{\partial G}{\partial S}\right|_P = 0 \qquad (23)$$

and,

$$\left.\frac{\partial G}{\partial P}\right|_S = 0 \qquad (24)$$

assuming that S and P are independent.

Applying equation (23) to equation (22) and solving for S yields,

$$S = (v_g/v_f)^{1/3} \quad . \qquad (25)$$

Thus for maximum flow rate S depends only on P.

When equations (25) and (22) are combined, a maximum G must satisfy equation (24). Equations (22), (25), and the state equation,

$$h_o = h_{f_o} + h_{fg_o}(s_o - s_{f_o})/s_{fg_o} \tag{26}$$

were programmed for saturated steam/water properties (16) and solved by digital computer for values of pressure which satisfied equation (24) for input values of P_o and h_o. Calculations showed that G has a single maximum value for known P_o and h_o. The maximum mass flux was thereby determined.

The results of the above computations are available in tabular form for use in RELAP4. The tables are entered with upstream volume stagnation pressure and junction stagnation enthalpy and a single mass flux is returned.

The Moody model is based upon an annular, two-phase, one-dimensional model with uniform axial velocity of each phase and thermodynamic equilibrium between phases. Additional assumptions are:

(1) Both phases experience the same local static pressure,

(2) The flow is isentropic from entrance to exit, hence stagnation enthalpy is constant,

(3) The liquid phase is incompressible, and

(4) The slip ratio and pressure are independent variables.

The Moody model is strictly applicable only in the saturated regime with stagnation pressure limits of 1 PSIA to 3000 PSIA. If the Moody model is used in the subcooled regime the code will enter the critical flow tables at zero quality.

2.4 THE HENRY- FAUSKE MODEL (12)

The Henry-Fauske model was developed primarily to account for the nonequilibrium nature of fluid flow under critical conditions and is applicable for fluids in the subcooled as well as the saturated and superheated states.

The derivation starts with the steady-state, one-dimensional continuity and momentum equations for two-phase flow;

Liquid continuity,

$$W_f v_f = A_f V_f \tag{27}$$

Vapor continuity,

$$W_g v_g = A_g V_g \tag{28}$$

Momentum,

$$-AdP = d(W_g V_g + W_f V_f)/g_c + dF_W \quad . \tag{29}$$

For high velocity flows the wall shear forces are negligible compared to the momentum and pressure gradient terms. Therefore, with the substitution of the liquid and vapor flow rate definitions, ($W_g = X\ W$ and $W_f = (1 - X)W$), equation (29) becomes,

$$-dP = Gd[XV_g + (1 - X)V_f]/g_c \quad . \tag{30}$$

It is assumed, for fixed upstream stagnation conditions, that X, v_g, v_f, V_g, and V_f are either constant or composite functions of P and z. Hence, equation (30) becomes,

$$G_j^{-1} = -\{\frac{d}{dP}[XV_g + (1 - X)V_f]/g_c\}_j \tag{31}$$

where the subscript j indicates that the enclosed quantities are evaluated at the junction. At critical flow, the mass flow rate exhibits a maximum with respect to junction pressure;

$$dG_c/dP|_j = 0 \quad . \tag{32}$$

Equation (32) can be applied to equation (31) to give an expression for the critical flow rate;

$$-G_C^{-2} = \{\frac{d}{dP}([XS + (1-X)][(1-X)Sv_f + Xv_g])/g_c S\}_j \qquad (33)$$

where, as before, S is defined by $S = V_g/V_f$. By taking the implied derivative, equation (33) can be expanded to

$$-G_C^{-2} = \{X[1+X(S-1)]dv_g/dP + S[1 + X(S-2)-X^2(S-1)]dv_f/dP$$

$$+ v_g[1 + 2X(S-1) + 2Sv_f(X-1) + S(1-2X)]dX/dP \qquad (34)$$

$$+ X(1-X)[v_f S - v_g/S]dS/dP\}_j/g_c S \quad .$$

Equation (34) can be simplified by using the following assumptions and relationships:

(1) The vapor and liquid velocities are equal (no slip);

$$S = 1 \qquad (35)$$

(2) The liquid phase is incompressible;

$$dv_f/dP = 0 \qquad (36)$$

(3) The vapor behavior can be described by a polytropic process such that,

$$dv_g/dP = v_g/nP \tag{37}$$

where n is the thermal equilibrium polytropic exponent derived by Tangren et al. (17) and given by,

$$n = [(1 - X)C_{V_f}/C_V + X]/[(1 - X)C_{V_f}/C_V + X/\gamma_g] \tag{37a}$$

(4) Negligible interphase mass transfer;

$$X_j = X_o \tag{38}$$

(5) The empirical result;

$$dS/dP|_j = 0 \quad . \tag{39}$$

Equations (35) through (39) serve to reduce equation (34) to

$$G_C = [X_o v_g/nP - (v_g - v_{f_o})dX/dP]_j^{-1/2} g_c^{1/2} \tag{40}$$

Formulating the actual junction fluid quality in terms of the equilibrium quality at that location and making use of empirical data as well as some mathematical manipulation, equation (40) becomes

$$G_c = g_c^{1/2} \{ X_o v_g / nP +$$

$$(v_g - v_{f_o})[\{(1 - X_o)N/s_{fg_E}\}ds_{f_E}/dP - \tag{41}$$

$$\{X_o C_{P_g}/Ps_{fg_o}\}(1/n - 1/\gamma)] \}_j^{-1/2}$$

The nonequilibrium parameter N is of primary import in the low quality regime. Based on experimental data (18), this parameter can be related to the equilibrium quality (X_{E_j}) as follows,

$$N(X_{E_j}) = \begin{cases} X_{E_j}/0.14 , & X_{E_j} < 0.14 \\ 1 , & X_{E_j} \geq 0.14 . \end{cases} \tag{42}$$

The relation for critical mass flux, equation (41), is coupled with the two-phase momentum equation;

$$(1-X_o)v_{f_o} P_o(1-R) + \gamma X_o P_o(v_{g_o} - Rv_{g_j})/(\gamma - 1)$$

$$= G^2[X_o v_{g_j} + v_{f_o}(1 - X_o)]^2/2g_c . \tag{43}$$

Solving equations (41) through (43) simultaneously generates the Henry-Fauske tables used in RELAP4. The tables are accessed with upstream volume stagnation pressure and junction stagnation enthalpy and the critical mass flux is returned.

Assumptions implicit in the use of this model are:

(1) System flow is isentropic and one-dimensional,

(2) The liquid phase is incompressible,

(3) The transfer of heat and mass between phases is negligible,

(4) Slip between phases is negligible and,

(5) At a junction the vapor phase expansion can be described by a polytropic process.

The Henry-Fauske model is applicable in the subcooled, saturated, and superheated regions with stagnation pressure limits of 1 PSIA to 2400 PSIA.

2.5 THE HOMOGENEOUS EQUILIBRIUM MODEL (HEM) (13)

This is essentially the same as the Sonic model described in section 2.2, page 15. It differs only in how it is utilized by the RELAP4 code. The HEM critical velocity and the Sonic model critical velocity are calculated using the same formula, equation (6). The HEM critical mass flux is then calculated from,

$$G = \{ \rho a \}_j \qquad (44)$$

The difference between the two models lies in how the density is calculated. In the Sonic model this density is computed from the upstream volume density by adjusting for

frictional losses and kinetic energy changes to the junction and by isentropic expansion from the Mach number just upstream of the junction to Mach one in the junction. In HEM the density is calculated by assuming that the upstream volume density and the pressure and enthalpy returned from the steam tables are stagnation properties. The junction density used in equation (44) is obtained by an isentropic expansion from the upstream volume assumed stagnation conditions to sonic velocity in the junction.

The assumptions inherent in the HEM are the same as for the Sonic model given on page 16 with the exceptions mentioned in the previous paragraph.

The HEM critical mass flux is also tabulated for use in RELAP4 for input values of upstream volume stagnation pressures and junction stagnation enthalpy. The Homogeneous Equilibrium model is applicable from 1 PSIA to 3000 PSIA.

2.6 THE MODIFIED MOMENTUM/HOMOGENEOUS EQUILIBRIUM MODEL (14)

The Modified Momentum/Homogeneous Equilibrium model (MM/HEM) is the same as the HEM model except when the quality is less than a user specified transition quality, X_T (the default value for this quality is $X_T = 0.02$).

As mentioned in Chapter One, the simple momentum or inertial flow solution is quite accurate at low junction pressure ratios but tends to exaggerate the flow rate as

critical conditions are approached. In order to compensate for this exaggeration the modified momentum model utilizes a correction to the downstream pressure based upon the retardation of vapor formation by the surface tension of the flashing fluid.

This more realistic downstream, or back pressure, is calculated from the empirical relationship,

$$P_b = C(1 - X_{UP}/X_T)^2 P_{SAT_{UP}} \tag{45}$$

where,

$$C = 1.0 - 0.284\ \sigma\ @\ P_{SAT_{UP}} / \sigma\ @\ P_{SAT_{200PSIA}} \quad . \tag{46}$$

In the subcooled region X_{UP} is set to zero and the critical flow rate is estimated from Bernoulli's equation with the pressure drop based on the modified back pressure, P_b ;

$$W = A[2g_c\ \rho\ (P_o - P_b)]^{1/2} \quad . \tag{47}$$

If, however, the modified back pressure is less than or equal to the downstream volume static pressure then the flow estimate is based on inertial considerations only. In the transition region ($0.0 \leq X < X_T$) the critical flow estimate is taken as the minimum of the flow rate predicted by equation (47) and the flow rate calculated from,

$$W_{MM/HEM} = G_{HEM} A (X_T / X_{UP})^{1/2} \quad . \tag{48}$$

The assumptions and limitations are the same as those for the HEM with the additional empirical assumption of equation (45).

2.7 JUNCTION FLOW RATE SOLUTION LOGIC

If one of the critical flow models is selected for a particular junction the flow rate solution process for that junction is accomplished as follows.

An inertial junction flow rate estimate is obtained from the following linearized expression derived from the integrated form of the momentum equation;

$$W_{t+\Delta t} = W_t + g_c (\Delta P - M W_t^2) \Delta t / I \tag{49}$$

where all of the parameters are evaluated at the junction.

This estimate is then compared with that for the particular critical flow model selected and the minimum identified. The fluid acceleration and junction friction required to force the actual calculated flow rate to the above identified minimum estimate is determined and the appropriate terms in the momentum equation are modified before simultaneous solution with the continuity and energy equations.

It is important to note that regardless of which critical flow model is selected, a comparison with inertial flow is always effected, regardless of the conditions in the junction and the upstream volume. Thus, if it is known apriori that a particular junction will not attain critical conditions, then selecting a critical flow model for that junction serves only to increase computer processing time. Additionally if, for example, the Moody critical flow model is selected for one of the junctions connecting core volumes, when the fluid in those core volumes becomes superheated near the end of the blowdown phase, the problem will abort because the Moody model is not applicable in the superheated regime.

3. OPTIMUM AREA RATIO DETERMINATION

3.1 INTRODUCTION

As reported in Section 1.5, the RELAP4 code in its present configuration, incorrectly computes stagnation properties. In order to alleviate this problem, the upstream volume flow area must be increased in order to prevent supersonic velocities from occurring in the volume immediately upstream from the break junction.

This chapter presents the results of a study done to determine the optimum area ratio (AR) (ie. break junction flow area/ upstream volume flow area) for this problem. The optimum area ratio was found to be 0.7 (ie. the flow area for volumes V5 and V21 must be increased from 3.67 to 5.24 square feet). In the chapters that follow, junctions, volumes, and heat slabs will be referred to by the letters J, V, and S, respectively, followed by the number of that junction, volume, or heat slab as defined in Figure 1 page 7. For example, J27 refers to the break junction on the vessel side of the break, V5 refers to the volume immediately upstream of break junction J27, and V21 refers to the volume immediately upstream of break junction J28.

3.2 GENERAL

This study made use of the Hope Creek BWR system as modeled for RELAP4 by EG&G Idaho, Inc. with Evaluation Model controls applied (RELAP4-EM). The input deck for this Evaluation Model is presented in Appendix A. The critical flow model required for the Evaluation Model is the Henry-Fauske model in the subcooled regime and the Moody model in the saturated regime. The other Evaluation Model controls are irrelevant to this area ratio study and discussion of these controls will be delayed until Chapter Four.

In order to understand the system transient response to be described in the following section, the control action inputs used in the problem must be explained.

The problem starts at time 0.001 seconds when the break occurs. At this time the break junctions J27 (vessel side) and J28 (pump side) are opened. At time 0.002 seconds, J25 (the pre-break recirculation flow junction) closes to complete the 200% break. Also at this time the feedwater valve, J30, closes, the two recirculation pumps, modeled by volumes V6 and V9, are shut off and begin to coast down, and a reactor SCRAM is initiated. At one second into the transient the main steam stop valve, J31, begins to close. This is a slow closing valve and is not fully closed until four seconds into the transient. The core spray system (CSS), J32, and the low pressure coolant injection system

(LPCIS), J33, actuate 26.5 seconds after the mixture level in the lower downcomer, V4, reaches 21.5 feet. As a reference, the bottom of the lower downcomer is 7.08 feet below the bottom of the active core. Flow through these systems does not begin, however, until the volumes to which they are discharging (V1 for the CSS and V10 for the LPCIS) depressurize to 304 PSIA and 310 PSIA, the rated discharge pressures of the CSS and LPCIS pumps, respectively. The automatic depressurization system (ADS), J26, is not activated until 120 seconds after the mixture level in the lower downcomer reaches 21.38 feet and thus is not a factor in this study.

In order to determine the optimum area ratio, six RELAP4 runs were completed with area ratios of 1.0, 0.9, 0.8, 0.7, 0.6, and 0.5. The temporal response of seven key parameters, listed below, to the imposed LOCA transient was studied;

1) Break flow rate, vessel side of break-J27,

2) Break flow rate, pump side of break-J28,

3) Core inlet flow-J29,

4) Lower downcomer-V4, mixture level,

5) Lower plenum-V11, pressure,

6) Clad surface temperature in the hottest (center) heat slab of the core-S23, and

7) Heat transfer coefficient of the fluid adjacent to the hot slab of the core-S23.

In general, the temporal parametric responses were bounded by the 1.0 and the 0.7 area ratio runs. For purposes of clarity only these two cases will be compared for all of the seven parameters considered. For break flow, J27, and core inlet flow, J29, all six cases will be compared for the time interval where the greatest (and most important) differences occurred.

In all of the figures presented in this chapter, the curves are identified by numbers (1.0, 0.9, 0.8, etc.) which correspond to the area ratio used to produce the data for that curve. The data used to produce the figures in this, and subsequent chapters, was extracted from the RELAP4 Plot/Restart tape rather than from the printed output. A Fortran IV program written to extract this data from the tape is presented in Appendix B.

3.3 ANALYSIS OF RESULTS

The most important parameter with respect to blowing down of the reactor vessel is the rate at which fluid exits the break. For a 200% break there are two break flows of significance; the flow from the vessel side of the break (J27) and the flow from the pump side of the break (J28).

Figure 3 shows the flow rate out of the vessel side of the break. When the break opens, the flow rate increases sharply, then decreases when the flow conditions become

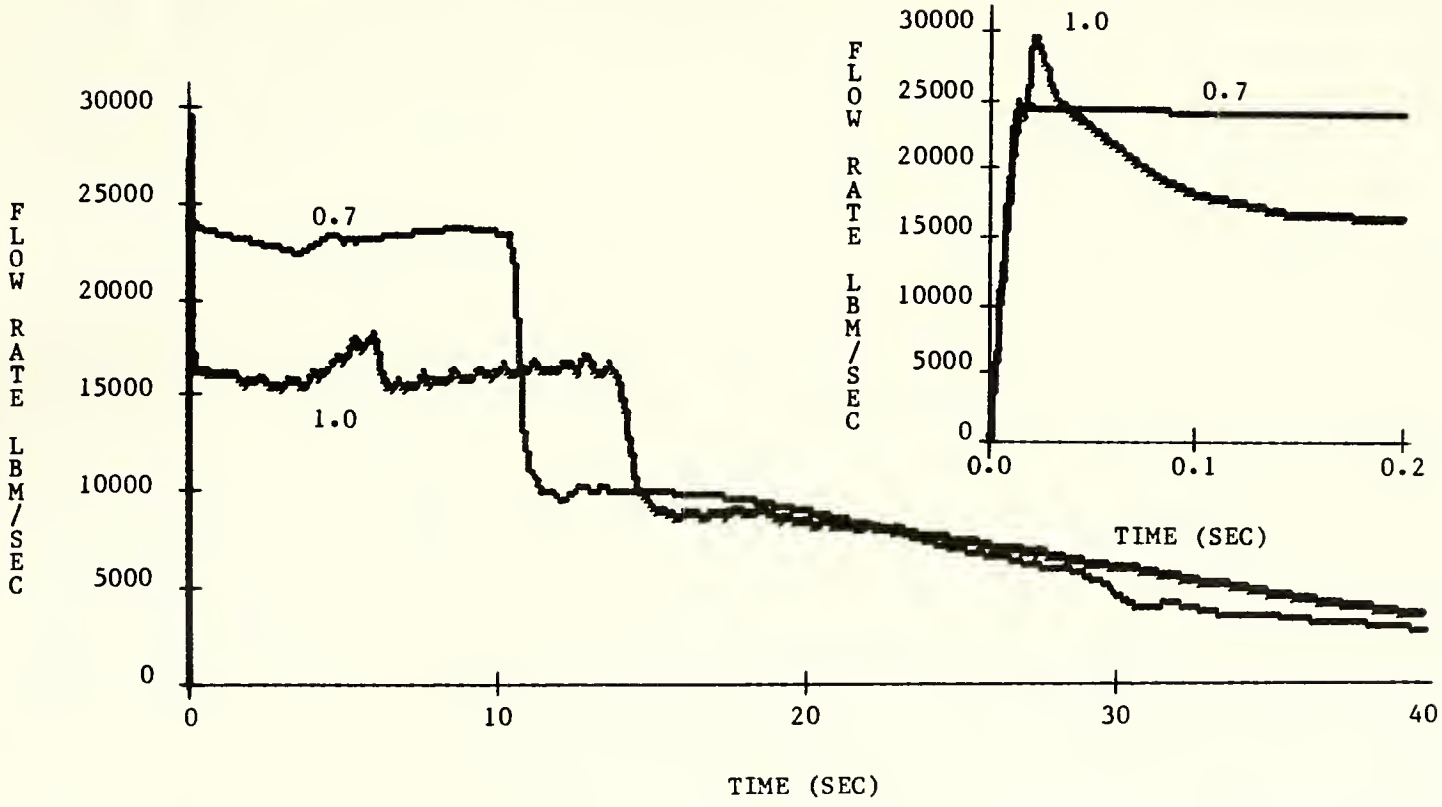

FIGURE 3
BREAK FLOW VESSEL SIDE OF BREAK (J27)
EVALUATION MODEL

critical, or choked. As the escaping fluid increases in steam quality, the flow rate decreases slightly until the main steam line closes at four seconds. The flow rate then increases momentarily. The flow rate remains relatively constant until the lower downcomer empties, allowing steam to escape from the break. As can be seen from Figure 4, the lower downcomer empties at about eleven seconds for the AR = 0.7 case and at about 14.5 seconds for the AR = 1.0 case. These times correspond to the sharp decreases in break flow seen in Figure 3. Following the emptying of the lower downcomer, the flow rate decreases steadily due to the gradual equilization of pressure between the containment and the reactor vessel.

The inset to Figure 3 reveals that the AR = 1.0 case initially peaks at a higher flow rate than does the AR = 0.7 case. As will be seen, similar results were obtained for initial break flow on the pump side of the break (Figure 6, page 42). A satisfactory explanation for this peculiar result could not be found. While the difference in this initial break flow is substantial, it occurs for such a short time that it is insignificant.

As can be seen, the major differences between the two runs lie in the value of the choked flow rate attained immediately following break initiation. For essentially the same driving pressure differential the AR = 0.7 case yields a break flow rate of about 23,000 LBM/SEC compared to only

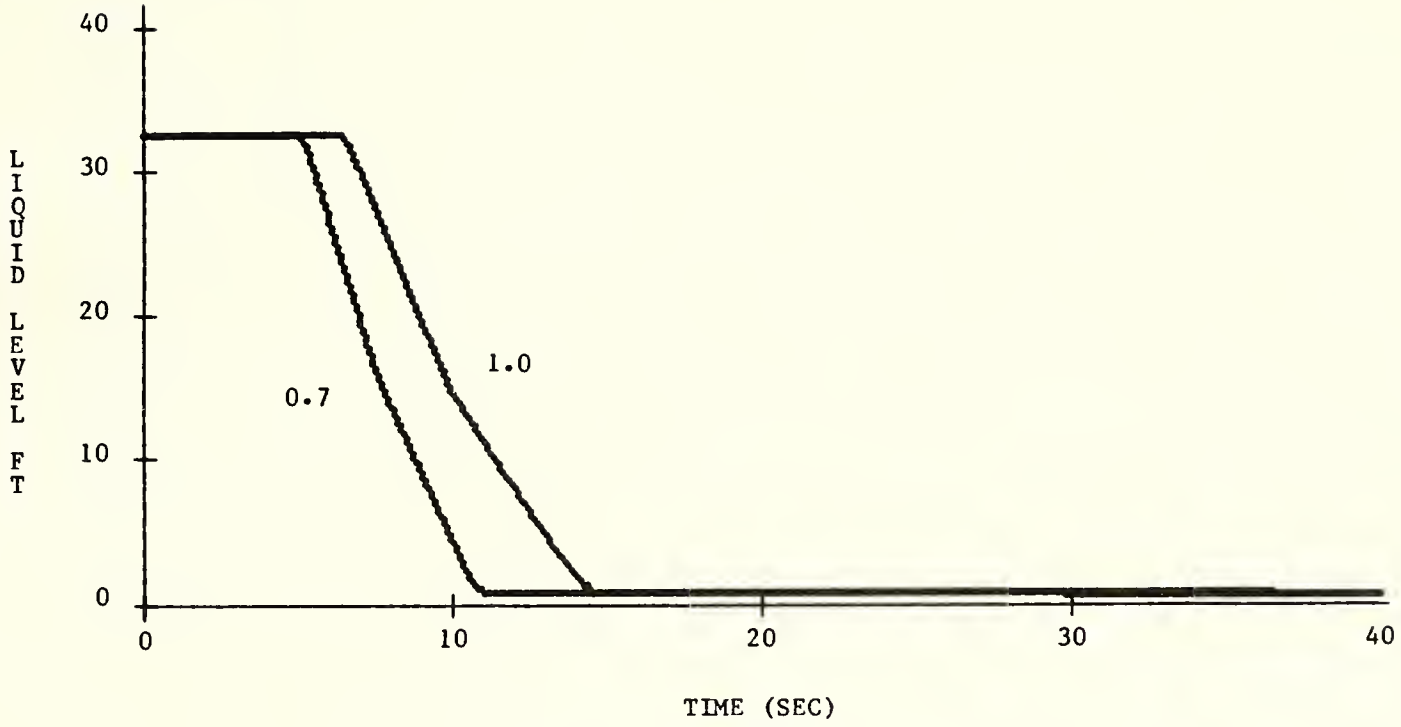

FIGURE 4
MIXTURE LEVEL IN LOWER DOWNCOMER (V4)
EVALUATION MODEL

16,000 LBM/SEC for the AR = 1.0 case. This results in the lower downcomer emptying faster for the AR = 0.7 case. After the lower downcomer empties, the two flow rates remain essentially the same, with the AR = 1.0 case being slightly greater due to the higher junction pressure differential which in turn is due to a lower break flow rate in the initial fourteen seconds of the blowdown.

Figure 5 shows the lower plenum pressure which is essentially the driving pressure for the break flow. This pressure decreases slowly during the first four seconds of the transient because the loss of water from the break and the loss of steam out of the main steam line are just slightly greater than can be compensated for by the production of steam in the core. After the main steam line closes at four seconds the pressure increases slowly until emptying of the lower downcomer allows steam to escape from the break. From here on the pressure decreases slowly as the reactor vessel and containment pressures equalize.

The differences between the two cases are due mainly to the time it takes for the lower downcomer to empty. Thus the AR = 1.0 case yields a higher maximum pressure due to the increased time between main steam line shutoff and emptying of the lower downcomer. Following the initiation of steam flow out of the break the two cases show depressurization rates which are essentially the same.

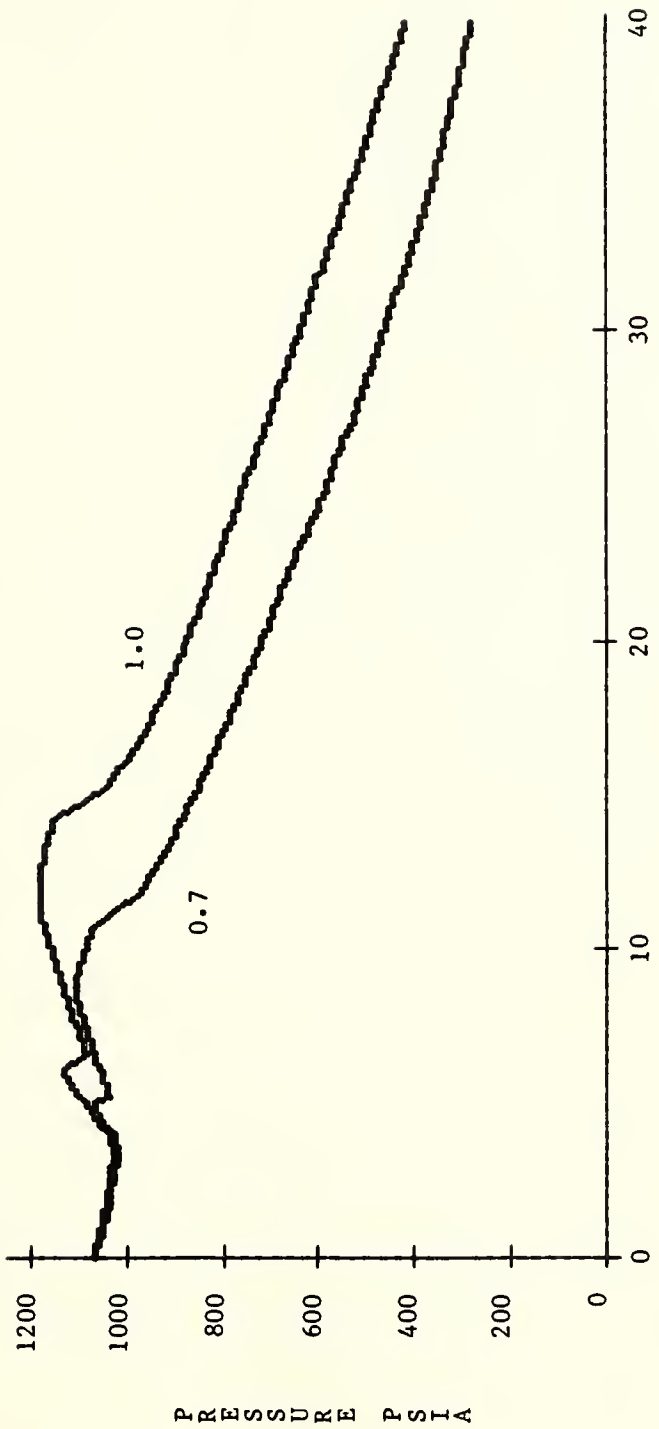

FIGURE 5
LOWER PLENUM PRESSURE (V11)
EVALUATION MODEL

The flow out of the pump side of the break (J27) is shown in Figure 6. It should be noted that J28 is modeled for a positive flow into the system. For convenience, Figure 6 is plotted showing positive flow out of the break. The flow characteristics on the pump side of the break are significantly different from those on the vessel side of the break due to the presence of the recirculation pump which begins to shut down at 0.002 seconds. The break flow initially increases at the same rapid rate as did the vessel side of the break and then decreases rapidly. This is because the flow is being restricted by the recirculation pump and the jet pump drive nozzles. After about 1.5 seconds the break flow (J28) decreases slowly and is oblivious to other changes in the reactor system.

As can be seen, the differences between the two cases shown in Figure 6 are slight. The inset in Figure 6 shows that the peak flow rate is about 20% higher for the AR = 1.0 case. As pointed out earlier, this difference is insignificant because it occurs for such a short period of time.

In all, it is apparent that the area ratio change had very little effect on the flow rate from the pump side of the break. This is due to the lower break junction velocity caused by the flow restrictions of the recirculation pump and jet pump drive nozzles.

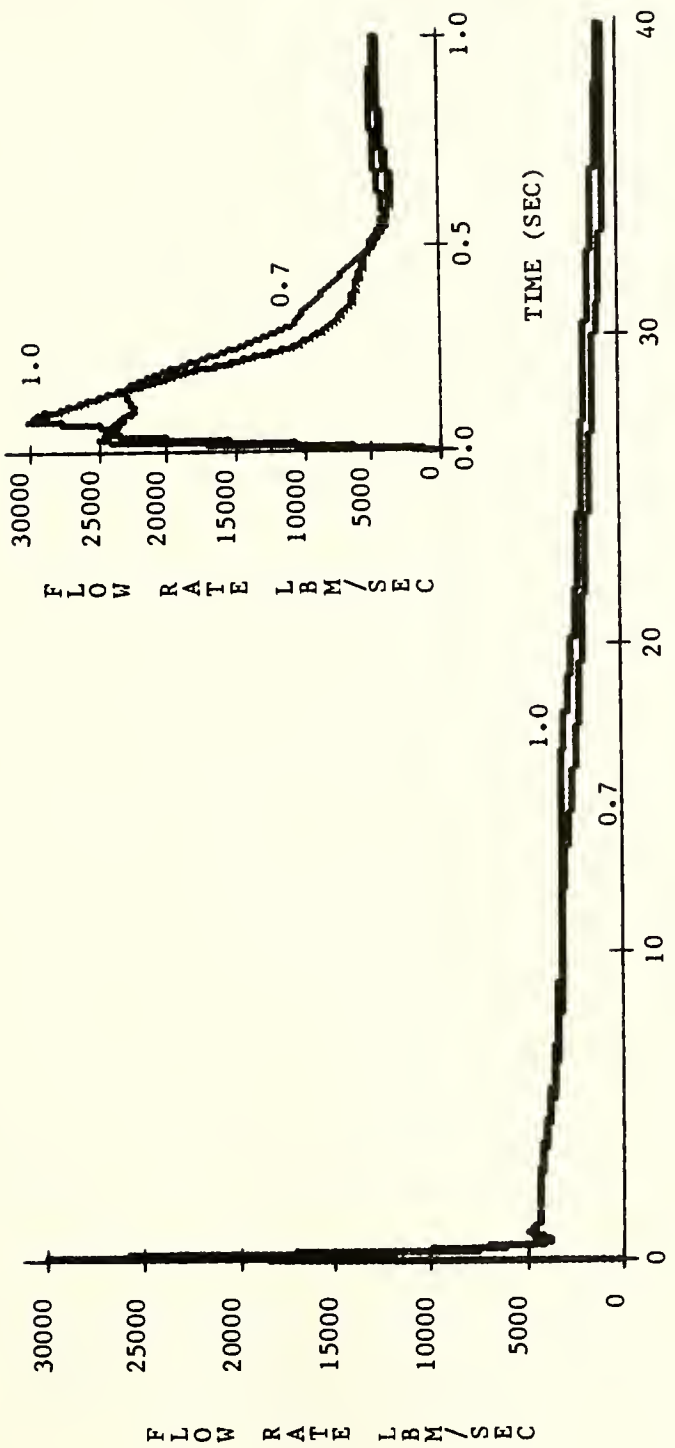

FIGURE 6
BREAK FLOW PUMP SIDE OF BREAK (J28)
EVALUATION MODEL

Figure 7 shows the core inlet flow (J29). Immediately after the break, the core flow begins to decrease as the recirculation pump on the side opposite the break coasts down and, as fluid normally flowing vertically upward through the core, is diverted to the break through the jet pump on the break side. This steady decrease continues until the jet pump intakes are uncovered. The jet pump intakes are located at the tops of volumes V19 and V20, and uncover when the mixture level in the lower downcomer reaches 15.7 feet. Reference to Figure 4, page 38, reveals that the jet pump intakes uncover at about eight seconds for the AR = 0.7 case and at about ten seconds for the AR = 1.0 case. These times correspond to the sharp decreases in core flow seen in Figure 7. Uncovering the jet pump intakes causes the remaining pressure differential across the core (due to the recirculation pump in the intact loop which is still coasting down) to diminish, and the core flow then reverses. At the time of core flow reversal, any liquid remaining in the core is replaced by steam from the upper plenum and the core dries out. The core flow remains negative until the water in the lower plenum begins to flash to steam as the system pressure drops to below saturation.

Flashing of the water in the lower plenum causes the lower plenum pressure to decrease at a slower rate than does the upper plenum pressure, thus the core inlet flow reverses again. The core flow then decreases as the liquid inventory

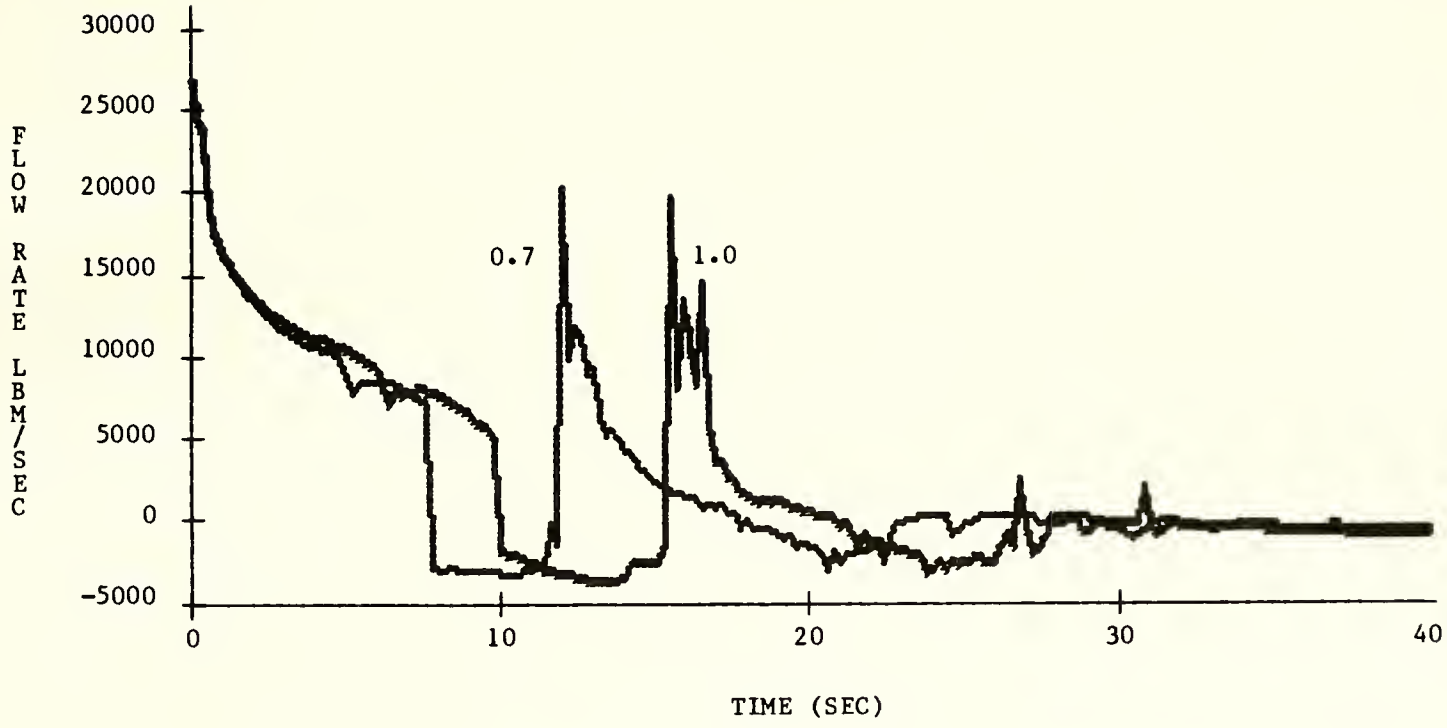

FIGURE 7
CORE INLET FLOW (J29)
EVALUATION MODEL

in the reactor system decreases. The flow again turns negative and remains near zero for the remainder of the transient.

The differences between the two cases can again be attributed to the differences in the initial break flow rates discussed earlier. The lower break flow rate for the AR = 1.0 case causes the jet pump drive nozzles to uncover later (ten seconds versus eight seconds), and thus the first core flow reversal occurs later. Lower plenum flashing starts when the system pressure drops below about 1000 PSIA, the saturation pressure for about 545 degrees F (the average water temperature in the lower plenum). Referring to Figure 5, page 40, the system pressure drops below 1000 PSIA at about 11.5 seconds for the AR = 0.7 case and at about sixteen seconds for the AR = 1.0 case. These times correspond to the second core reversals seen in Figure 7.

The temporal response of clad surface temperature is shown in Figure 8. The data for this graph is obtained by taking the surface temperature of the hottest heat slab (S23), which is in the center of the core. It should be noted that this system is modeled with the core heat slabs representing an average fuel assembly. Thus the surface temperature of heat slab S23 represents the hottest fuel clad temperature of an average fuel assembly.

A more accurate core model, such as the model by Hendrix (9), divides the core into two regions, one

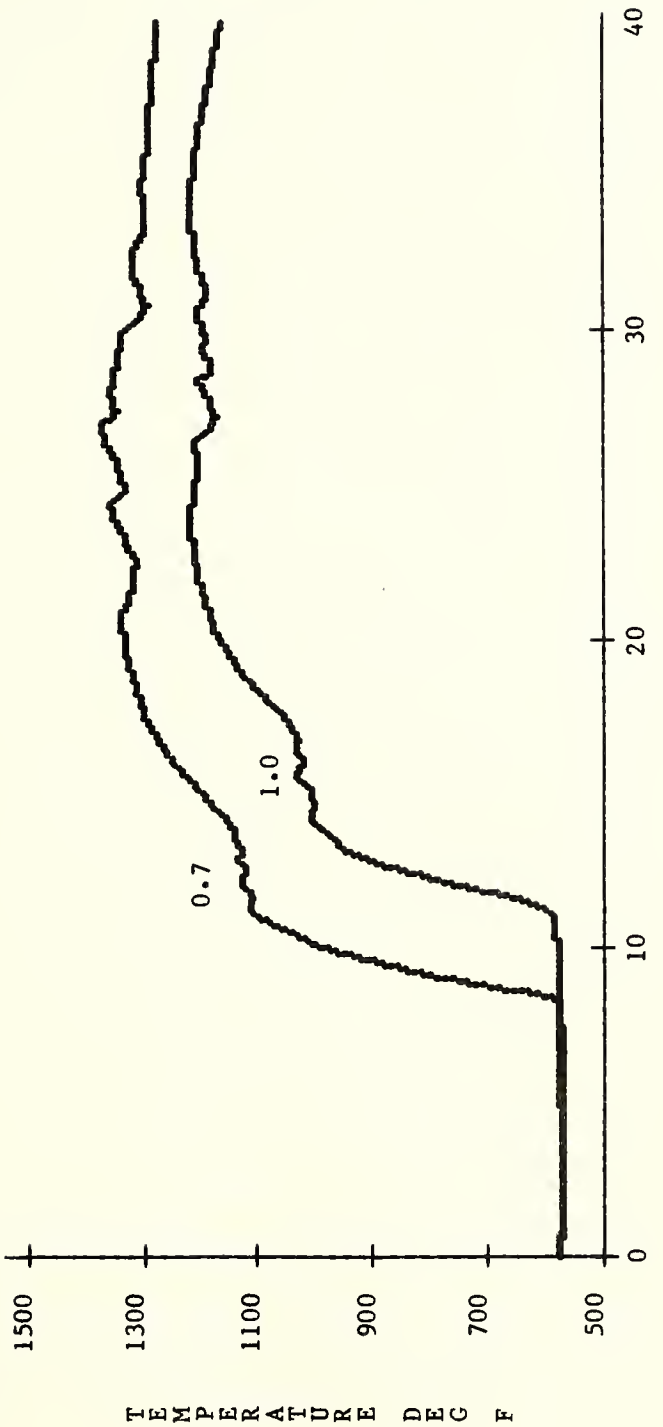

FIGURE 8
CLAD SURFACE TEMPERATURE (S23)
EVALUATION MODEL

representing the average fuel assembly, and the other representing the hot fuel assembly. While this more sophisticated model will more accurately predict core temperatures, it will also increase computer processing time and would have added little to this analysis, which is concerned with relative, rather than absolute, parametric responses.

Figure 8 indicates that initially the clad surface temperature follows the fluid saturation temperature (approximately 565 degrees F) closely until the steam quality in the core becomes appreciable. At the time of first core flow reversal the temperature of the cladding surface increases sharply as the core dries out and the heat transfer coefficient of the fluid adjacent to the heat slab decreases. Figure 9 shows the heat transfer coefficient (HTC) of the fluid adjacent to S23. The HTC decreases slowly until the first core flow reversal where it drops to nearly zero due to dryout of the core. The time for this sharp decrease in the HTC corresponds to the time of first core flow reversal (Figure 7) and to the sharp increase in clad surface temperature (Figure 8). Refering back to Figure 8, the clad surface temperature continues its rapid increase until the time of lower plenum flashing and second core flow reversal. There it levels out somewhat due to the liquid flow through the core caused by lower plenum flashing. Following the flow spike caused by lower plenum

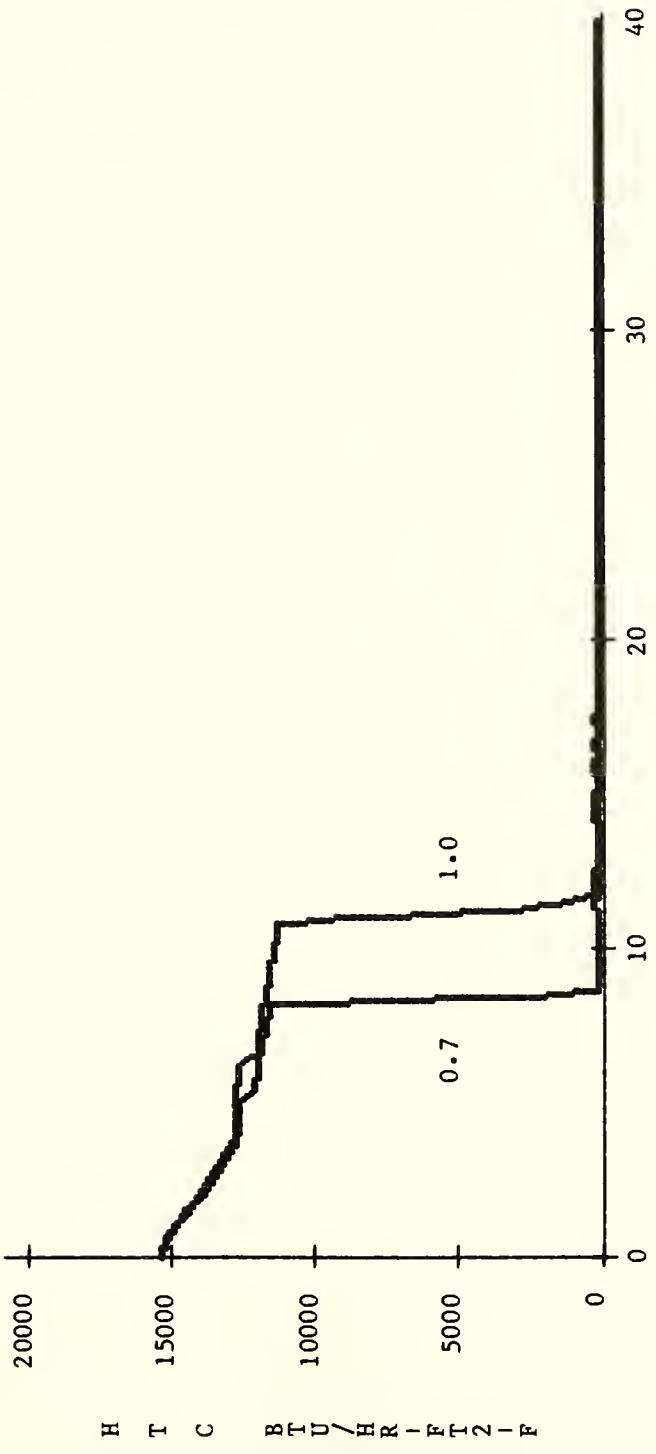

FIGURE 9
HEAT TRANSFER COEFFICIENT IN HOT SLAB (S23)
EVALUATION MODEL

flashing the surface temperature of the cladding again increases, levels out, and remains relatively constant until the core spray system (CSS) becomes effective. (The CSS does not become effective in the forty seconds of transient time shown).

As shown by Laird (19) and Bruch (20) if the transient is allowed to progress beyond forty seconds, the clad surface temperature will gradually decrease until about 125 seconds, when it will begin to increase. The peak cladding temperatures will not be reached until well into the reflood phase of the accident. RELAP4-FLOOD is not available for BWR s and therefore the peak cladding temperature cannot be predicted using RELAP4 in its present configuration.

Again, the differences between the AR = 0.7 clad surface temperature case and the AR = 1.0 case lie in the initial break flow differences which directly influence the time of first core flow reversal (Figure 7). As pointed out, the times of first core flow reversal correspond to drying out of the core and to the resultant sharp increases in cladding surface temperature seen in Figure 8. Following first core flow reversal the clad surface temperature for both cases follow nearly the same trends with the AR = 1.0 case remaining below the AR = 0.7 case.

3.4 OPTIMUM AREA RATIO SELECTION

Figure 10 shows the break flow from the vessel side of the break for each of the area ratio cases studied. In order to accentuate the differences between the cases, the transient response is only shown for the transient time from one to ten seconds.

As can be seen from Figure 10, increasing the upstream volume flow area (ie. decreasing the area ratio) results in increasing the break flow rate, with the slight exception of the time period from five to ten seconds for the AR = 0.5, 0.6, and 0.7 cases. While these three cases are different for most of the transient shown, they never differ by more than four percent, and for all practical purposes can be considered to be the same.

Similar results are obtained for core inlet flow shown in Figure 11 for transient times from two to eleven seconds. The main point of interest is the time of first core flow reversal which occurs earlier as the area ratio is decreased until the area ratio reaches 0.7. Further reductions in area ratio produce no significant changes.

As pointed out in the introduction to this chapter, the parametric responses studied generally fell between the AR = 1.0 case and AR = 0.7 case. It was also noted that results similar to those demonstrated by Figures 10 and 11 were observed for all of the parameters studied (ie. decreasing

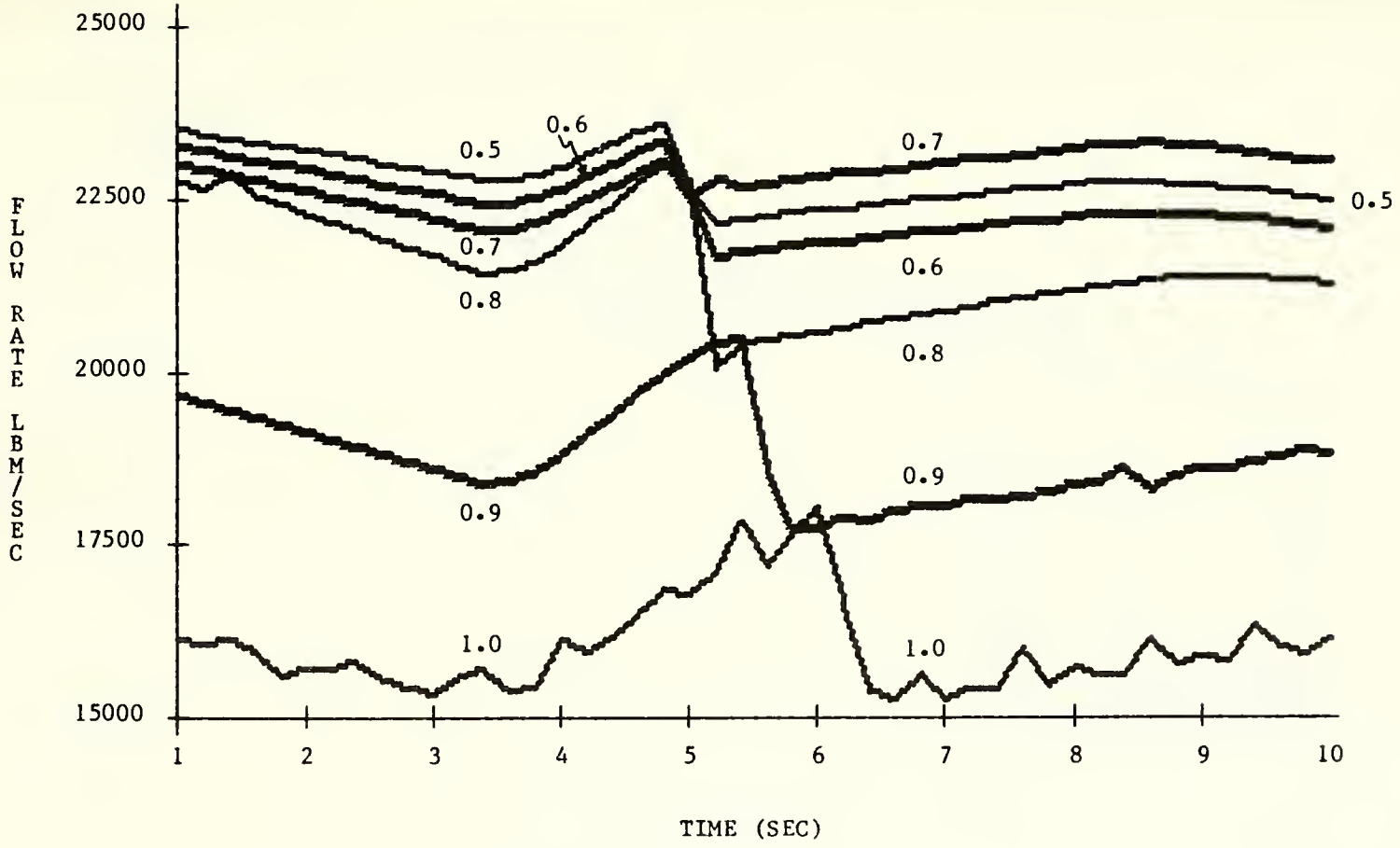

FIGURE 10
BREAK FLOW VESSEL SIDE OF BREAK (J27)
EVALUATION MODEL

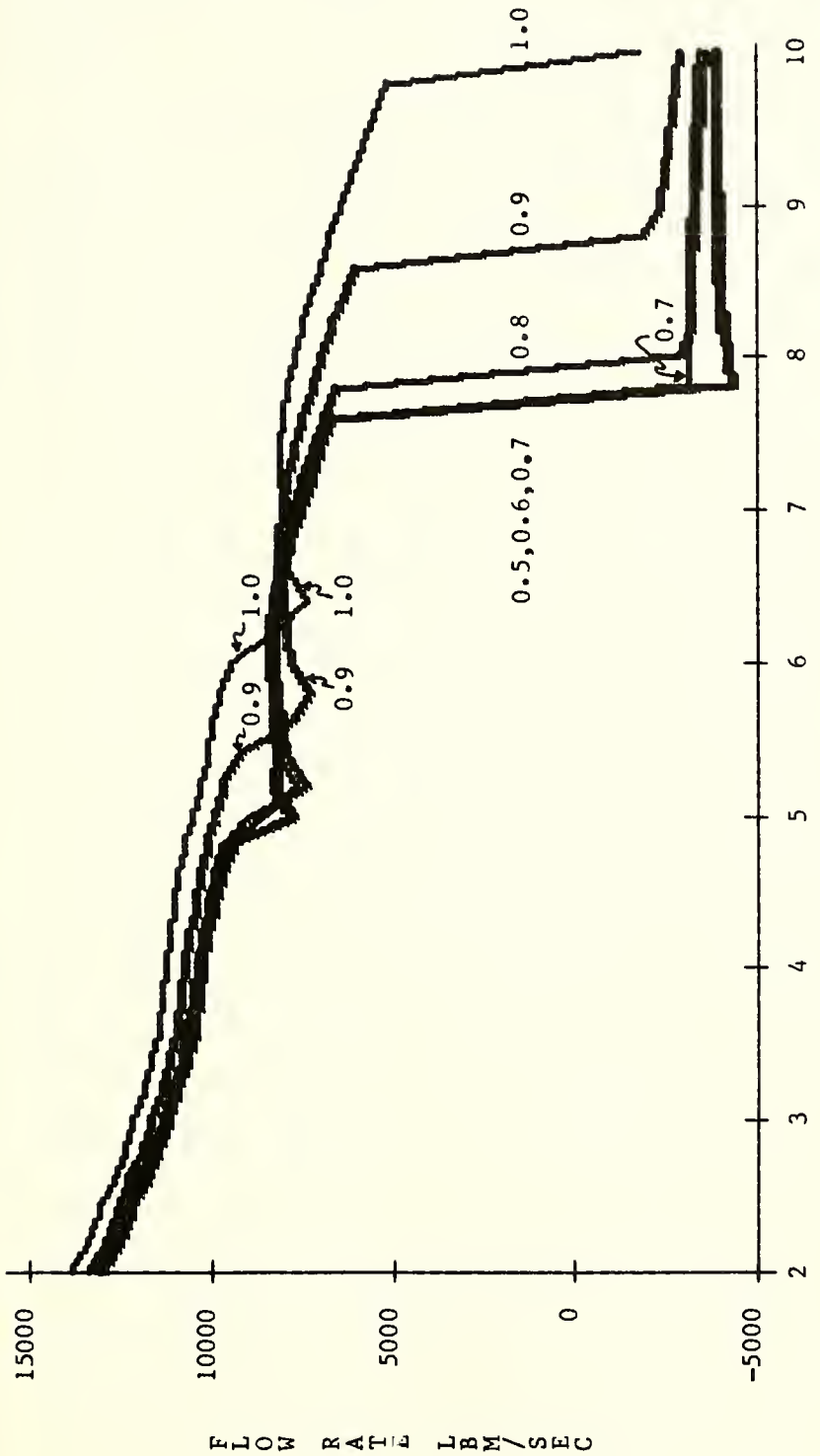

FIGURE 11
CORE INLET FLOW (J29)
EVALUATION MODEL

the area ratio below 0.7 resulted in no significant change in the response of the parameter). For these reasons, an area ratio of 0.7 was chosen as the optimum value for this problem.

It is important to note that using the RELAP4 code without correcting for the stagnation properties calculation error (ie. using AR = 1.0) yields results which are not conservative. That is, low break flow rates and low clad surface temperatures are predicted.

4. CRITICAL FLOW MODEL SENSITIVITY STUDY

4.1 INTRODUCTION

A sensitivity study of the critical flow models discussed in Chapter Two using the Standard Model (best estimate) configuration of the RELAP4 code (RELAP4-SM) was made. A comparison was also made with the Evaluation Model (RELAP4-EM). It should be recalled that the critical flow model for the Evaluation Model is the Henry-Fauske model in the subcooled regime and the Moody model in the saturated regime. The input data decks used in this study are discussed in Appendix A.

The results of the area ratio study presented in the previous chapter were applied to the sensitivity study runs. That is, the flow areas for volumes V5 and V21 (the volumes immediately upstream from the break junctions, J27 and J28, respectively) were increased from 3.67 to 5.24 square feet. The Evaluation Model run presented in this chapter is the AR = 0.7 case from Chapter Three.

4.2 ANALYSIS OF RESULTS

Figure 12 shows the break flow rate, for the first twenty seconds of the transient, from the vessel side of the

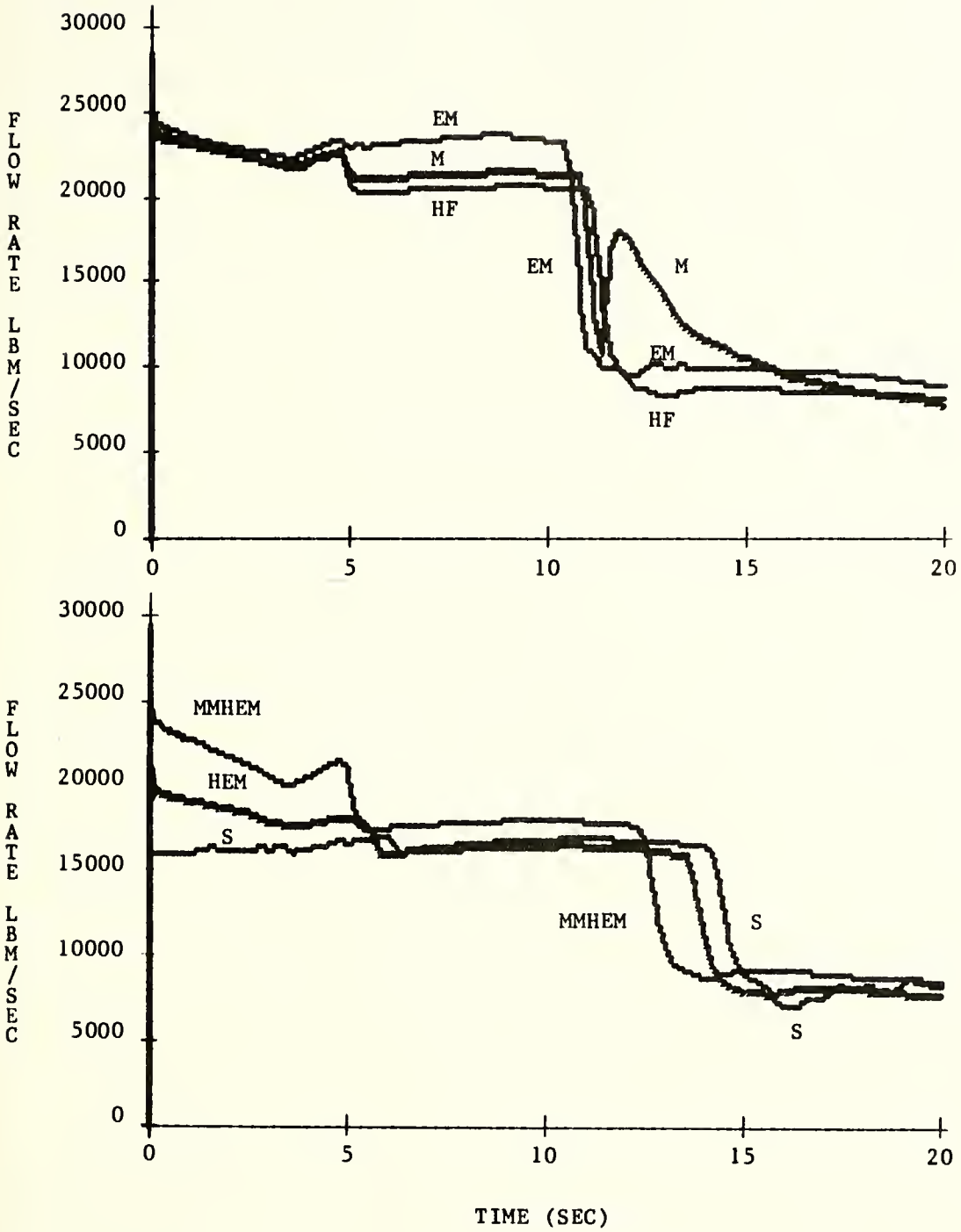

FIGURE 12
BREAK FLOW VESSEL SIDE OF BREAK (J27)

break (J27) for the six cases studied. The transient response for this parameter is uninteresting from twenty to forty seconds and is similar to the response shown in Figure 3, page 36. In Figure 12, and in the figures and discussion that follows, the different cases are identified by the symbology presented in Table 2.

TABLE 2. CRITICAL FLOW MODEL SYMBOLOGY

CRITICAL FLOW MODEL	SYMBOL
SONIC	S
HOMOCENEOUS EQUILIBRIUM	HEM
MODIFIED MOMENTUM/HOMOGENEOUS EQUILIBRIUM	MMHEM
HENRY-FAUSKE	HF
MOODY	M
EVALUATION MODEL	EM

Figure 12 reveals that the EM yields the highest average break flow rate for the initial period of the blowdown, and is followed by the Moody, the Henry-Fauske, the MMHEM, the HEM, and the Sonic models.

With the execption of the Moody model, the results depicted in Figure 12 are as would have been expected based

on the discussion on break flow given in Chapter Three. That is, following the rapid decrease in break flow characteristic of all of the models at about eleven seconds, the Moody model exhibits a peculiar jump in break flow at about 11.5 seconds.

Analysis of the Moody data indicates that the lower downcomer empties at 11.2 seconds, allowing steam to escape from the break. At 11.6 seconds, the lower downcomer refills to a level of about 1.2 feet, and the flow out of the break again becomes mostly liquid. The lower downcomer empties again at 12.6 seconds, and remains empty for the remainder of the transient. This oscillation of lower downcomer water level is caused by increased steam generation in the core starting at about 11.4 seconds. The increased steam generation forces water from the lower plenum, through the jet pump intakes, and into the lower downcomer. The increase in core steam generation rate is caused by a return to nucleate boiling following first core flow reversal and core dryout. The return to nucleate boiling will be explained in the discussion of the heat transfer coefficient which follows.

The oscillation of lower downcomer mixture level, described above for the Moody model, does not occur for the other five cases.

The break flow from the pump side of the break (J28) showed only slight differences (less than two percent)

between the six cases studied. All six cases were very similar to the response shown in Figure 6, page 42, and thus are not presented.

Table 3 shows the times for uncovering the jet pump drive nozzles and the times for emptying of the lower downcomer for the six cases studied. (Recall from Chapter Three that the jet pump drive nozzles uncover when the mixture level in the lower downcomer reaches 15.7 feet, which corresponds to a mixture level of about 8.6 feet in the active core). The times presented in Table 3 are a direct result of the initial break flow rates depicted in Figure 12.

TABLE 3. TIME TO UNCOVER JET PUMP DRIVE NOZZLES AND TO EMPTY LOWER DOWNCOMER

CRITICAL FLOW MODEL	TIME(SEC) TO UNCOVER JET PUMP DRIVE NOZZLES	TIME(SEC) TO EMPTY LOWER DOWNCOMER
EM	7.5	10.8
M	7.6	11.2
HF	7.7	11.4
MMHEM	8.1	12.8
HEM	8.8	14.0
S	9.8	14.6

As discussed in Chapter Three, the time that the jet pump drive nozzles uncover should correspond to the time of first core flow reversal, and the time that the lower downcomer empties should correspond to the time of second core flow reversal. This is indeed the case, as can be seen in Figure 13, which shows the core inlet flow (J29) for the six cases studied from zero to twenty seconds into the transient. The remainder of the transient was similar to the EM response shown in Figure 7, page 44. That is, the core flow remained near zero with small oscillations due to varying core steam generation rates.

The transient responses seen in Figure 13 are as would have been expected from the discussion on core inlet flow given in Chapter Three, again with the exception of the Moody model. The relatively small flow spike at the time of second core flow reversal for the Moody case is due mainly to the return to nucleate boiling discussed earlier. This return to nucleate boiling results in increased amounts of steam being generated in the core which counteracts the effects of lower plenum flashing on core differential pressure. The end result is the smaller flow spike seen at the time of second core flow reversal in Figure 13.

Figure 14 shows the heat transfer coefficient (HTC) at the hottest heat slab in the core for the six cases studied. It should be noted that, while the HTCs depicted in Figure 14 are for the hottest heat slab in the core, for the HEM,

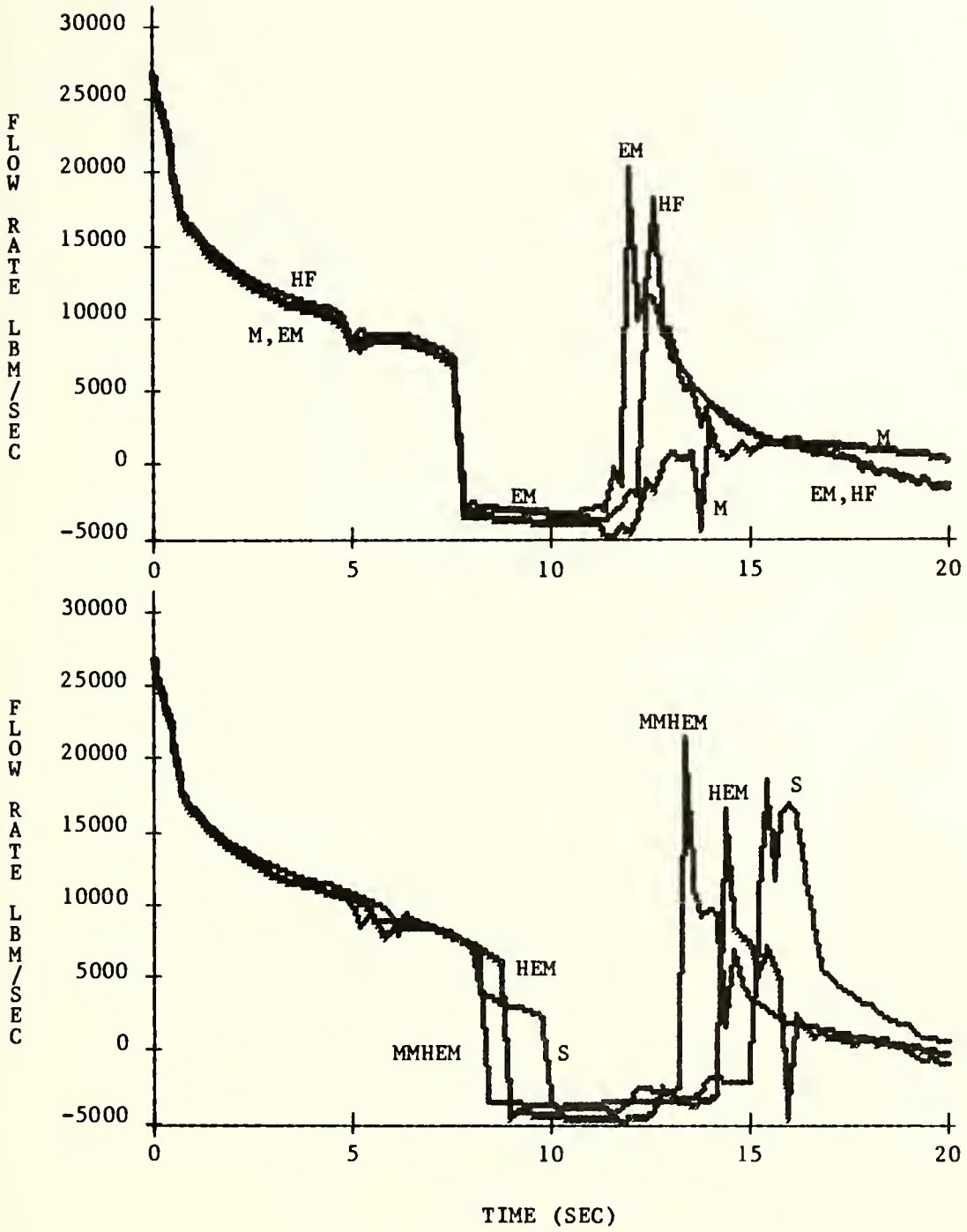

FIGURE 13
CORE INLET FLOW (J29)

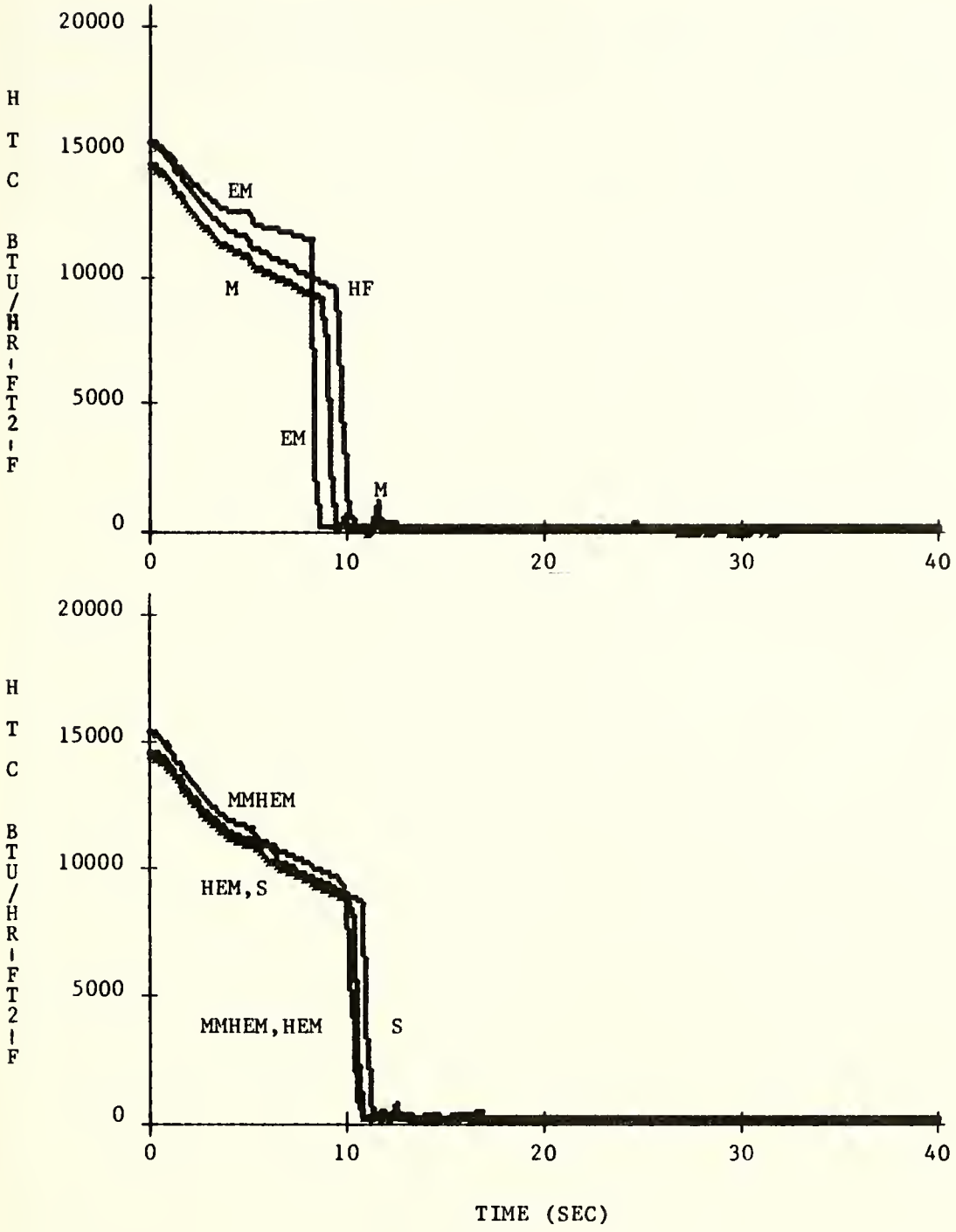

FIGURE 14
HEAT TRANSFER COEFFICIENT
HOTTEST CORE HEAT SLAB

Sonic, and Moody models the hottest heat slab turned out to be heat slab S24 (the slab immediately above the center heat slab, S23) and for the other three models S23 was the hottest heat slab. This result is explained as follows.

One of the main differences between the Evaluation Model (RELAP4-EM) and the Standard Model (RELAP4-SM) is in the heat transfer logic used in the two cases. For the case of RELAP4-EM, it is stated in Appendix K to 10 CFR 50 that "after critical heat flux is first predicted at an axial fuel rod location during blowdown, the calculation shall not use nucleate boiling heat transfer correlations at that location subsequently during the blowdown even if the calculated local fluid and surface conditions would apparently justify the re-establishment of nucleate boiling". RELAP4-SM, on the other hand, allows re-establishment of nucleate boiling if the conditions warrant. For the HEM, Sonic, and Moody model cases, at the time of first core flow reversal, the conditions were such that nucleate boiling was re-established at heat slab S23, while film boiling continued at heat slab S24. Nucleate boiling conditions persisted for about ten seconds at heat slab S23 for both the HEM and Sonic models and for about three seconds for the Moody model. This resulted in the temperature of heat slab S23 being lower than that for heat slab S24 in all three cases for the remainder of the transient.

Figure 15 shows the cladding surface temperature at the hottest heat slab in the core for the six cases studied. Again, for the HEM, Sonic, and Moody model cases, the hottest heat slab was S24, while for the other three cases S23 was the hottest.

Table 4 shows the peak cladding surface temperature attained during the blowdown for each of the six cases studied.

TABLE 4. PEAK CLADDING SURFACE TEMPERATURE

CRITICAL FLOW MODEL	PEAK CLADDING SURFACE TEMPERATURE (DEG F)
EM	1349
HF	919
M	909
MMHEM	898
HEM	850
S	846

As can be seen from Figure 15 the surface temperature decreases rapidly for the Moody model case at about eleven seconds. This decrease corresponds to the re-establishment

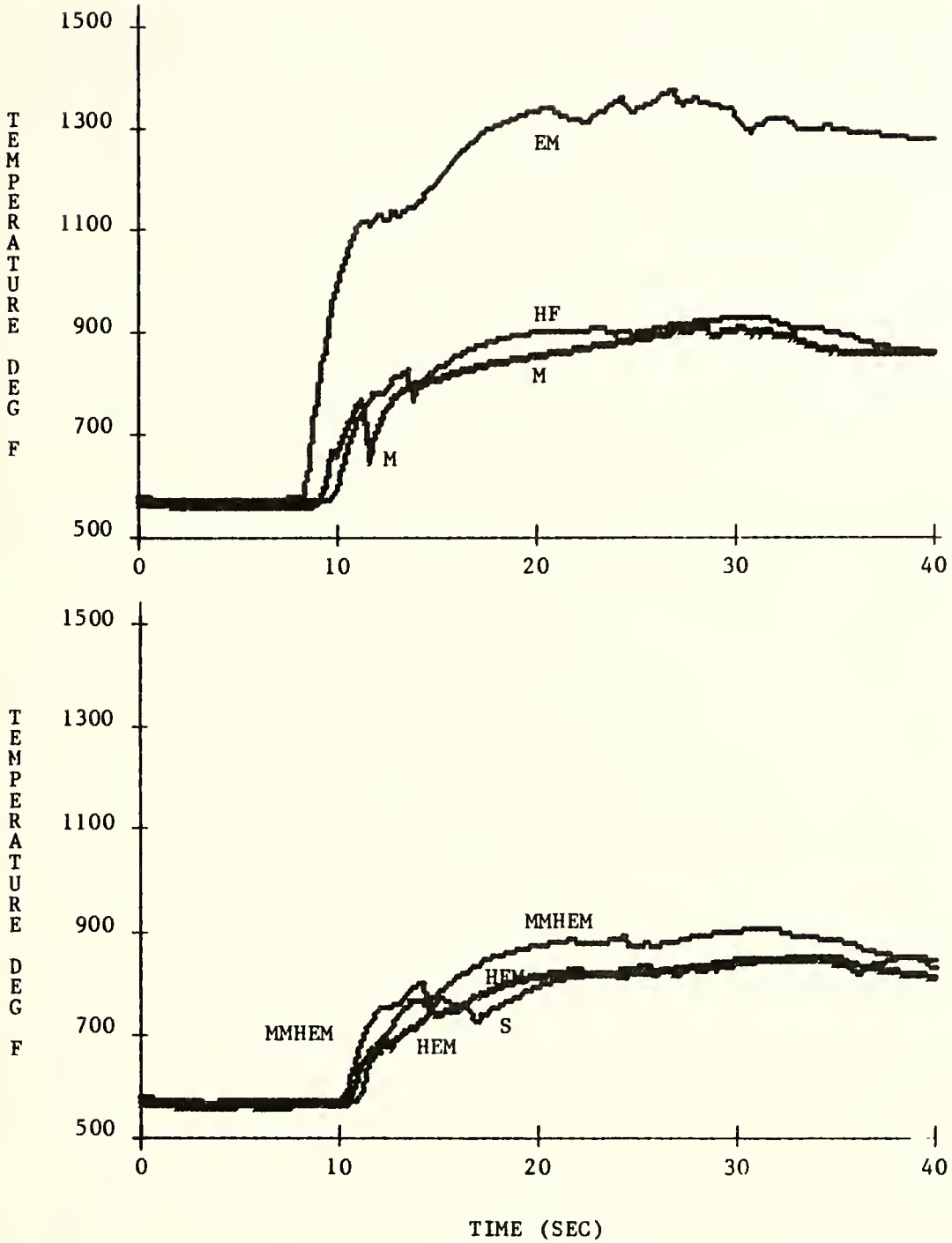

FIGURE 15
CLAD SURFACE TEMPERATURE
HOTTEST CORE HEAT SLAB

of nucleate boiling which, for this model only, occurs in heat slab S24, as well as in heat slab S23. This return to nucleate boiling at heat slab S24 is characterized by the slight increase in the HTC seen at about eleven seconds in Figure 14. With the exception of this one peculiarity for the Moody model, the surface temperature transient responses for all six cases follow trends that are consistent with the discussion of clad surface temperature in Chapter Three.

4.3 CONCLUSIONS

From the analysis of the previous section it is apparent that the Evaluation Model, as expected, produced the most conservative results. As pointed out, this is primarily due to the different heat transfer logic in the RELAP4-EM and RELAP4-SM configurations.

Based on initial break flow rate (Figure 12, page 55) it is clear that the Moody model is most conservative, followed by Henry-Fauske, MMHEM, HEM, and Sonic. Note, however, that the Moody and Henry-Fauske models differ by only about five percent.

Based on peak cladding surface temperature attained (Table 4, page 63) one would conclude that the Henry-Fauske model is more conservative than the Moody model, followed by the other models in the same relative order as above. Note again, that the difference between the Moody and Henry-Fauske models is slight (only about one percent).

For these reasons, the Moody and Henry-Fauske models are rated as equivalent based on conservative results, followed, in order of their relative degrees of conservatism, by the MMHEM, the HEM, and the Sonic critical flow model.

5. SUMMARY

5.1 RESULTS

This study utilizes the RELAP4/MOD5 Computer Code to analyze the effects of critical flow modeling on the thermal-hydraulic transient response of a General Electric boiling water reactor to a major primary coolant line rupture. Included in the study is a presentation of the equations, assumptions, and limitations of the critical flow models available for use in RELAP4. Additionally, an evaluation of a temporary solution to a RELAP4 coding error associated with stagnation properties calculation is presented.

The results of this investigation indicate that:

(1) A solution to the stagnation properties calculational error that exists in the RELAP4 code, when applied to the Evaluation Model, (RELAP4-EM) provides a conservative evaluation, relative to the Standard Model (RELAP4-SM), regardless of which of the five critical flow models available in the code is selected;

(2) Of the five critical flow models available for use in RELAP4, the Moody model and the Henry-Fauske model are nearly equivalent in their relative degrees of conservatism. Following these models, in order of relative degree of conservatism, are the Modified Momentum/Homogeneous

Equilibrium model, the Homogeneous Equilibrium model, and the Sonic model;

(3) In order to best alleviate the stagnation properties coding error, the flow areas for the volumes immediately upstream from the recirculation line rupture should be increased such that the area ratio (break flow area / upstream volume flow area) is 0.7.

All of the critical flow models in RELAP4, with the exception of the Sonic model, require the use of stagnation properties for estimation of flow rate under critical or choked conditions. The RELAP4 code, in its present form, incorrectly computes stagnation properties when the flow rate is such that the code predicts supersonic velocities in the volume immediately upstream of the junction where critical flow conditions exist. The results of this investigation indicate that the optimum solution to this problem is to arbitrarily increase the upstream volume flow area such that the area ratio is 0.7.

The Hope Creek boiling water reactor, included as a sample problem in the RELAP4 Users Manual, was used to analyze the effects of critical flow modeling on the predicted blowdown response of this BWR to a double-ended guillotine rupture of the primary coolant recirculation line. Applying the above mentioned stagnation properties calculation problem "fix" to RELAP4-EM provides a conservative evaluation relative to RELAP4-SM, regardless of

which of the five critical flow models available in the code is selected. Applying the "fix" to the Standard Model it was found that the Moody and Henry-Fauske critical flow models provide nearly equivalent evaluations in terms of peak cladding temperatures attained during the blowdown. The other three critical flow models, in order of their relative degrees of conservatism, were found to be the Modified Momentum/Homogeneous Equilibrium model, the Homogeneous Equilibrium model, and the Sonic model.

5.2 RECOMMENDATIONS FOR FURTHER STUDY

Based on this investigation the following recommendations for future research are presented:

(1) While this investigation rated the critical flow models by their relative degree of conservatism, comparison of the results of RELAP4 analysis with LOFT, SEMISCALE, or other large scale experimental data would provide valuable insight as to which of the models most accurately predict flow rate under critical or choked conditions.

(2) The heat transfer logic employed by the RELAP4 code appears to have a very significant effect on the overall performance of the code. Analysis of the effects of changing heat transfer and critical heat flux correlations would be invaluable to future users of the code.

REFERENCES

1) Acceptance Criteria for Emergency Core Cooling Systems for Light-Water Nuclear Power Reactors. 10 CFR 50, Federal Register 39, No. 3, January 1974.

2) Ibid., Appendix K, p. 164a.

3) Laird, R. E. An Investigation of the RELAP4/MOD5 Computer Code and its Applicability to General Electric Boiling Water Reactors, An M.S. Thesis in Nuclear Engineering, The Pennsylvania State University, 1978.

4) Slifer, C. and J. E. Hench. Loss-of-Coolant Accident and Emergency Core Cooling Models for General Electric Boiling Water Reactors, NEDO-10329, p. 3, April 1970.

5) Bruch, C. G. (ed.) RELAP4/MOD5: A Computer Code for Transient Thermal-Hydraulic Analysis of Nuclear Reactors and Related Systems, Users Manual, Vol. I-III. ANCR-NUREG-1335, September 1976.

6) Ardon, K. H. and R. A. Furness. A Study of the Critical Flow Models Used in Reactor Blowdown Analysis. Nuclear Engineering and Design, 39, pp. 257-266, 1976.

7) Bruch, op. cit., p. I-145.

8) Laird, op. cit., p. 108.

9) Hendrix, C. E. Hope Creek BWR Evaluation Model. PG-R-05-77, p. 2, February 1977.

10) Bruch, op. cit., p. I-149.

11) Moody F. J. Maximum Flow Rate of a Single-Component Two-Phase Mixture, Journal of Heat Transfer, ASME, 87, p. 134, February 1965.

12) Henry R. E. and H. K. Fauske. The Two-Phase Critical Flow of One-Component Mixtures in Nozzles, Orifices, and Short Tubes, Journal of Heat Transfer, ASME, 93, p. 179, May 1971.

13) Hutcherson M. N. Contribution to the Theory of Two-Phase Blowdown Phenomenon, ANL/RAS 75-42, p. 265, November 1975.

14) Bruch, op. cit., p. I-183.

15) Ibid., p. I-147.

16) Keenan J. H. and F. G. Keys. Thermodynamic Properties of Steam, John Wiley and Sons, Inc., New York, N.Y., First Edition, 1955.

17) Tangren R. F. et al. Compressibility Effects in Two-Phase Flow. Journal of Applied Physics, Vol. 20, p. 736, 1949.

18) Starkman E. S. et al. Expansion of a Very Low Quality Two-Phase Fluid Through a Convergent-Divergent Nozzle. Journal of Basic Engineering, Trans. ASME, Series D, Vol. 86, No. 2, p. 247, June 1964.

19) Laird, op. cit., p. 114.

20) Bruch, op. cit., p. III-136.

21) Physical Record Length and Fill Buffer Subroutine. The Pennsylvania State University Computation Center, Revised February 1976.

APPENDIX A

INPUT DATA DECKS

This appendix provides a listing of the input data decks for the Evaluation Model (RELAP4-EM) and the Standard Model (RELAP4-SM) used in this investigation. The data consists of title cards, data cards, and comment cards. The comment cards are prefixed with an asterisk (*).

Table 5 is the input deck for RELAP4-EM that was used in the area ratio study presented in Chapter Three. The only two cards that were changed to produce the different area ratio runs were the volume data cards 050051 and 050211. Card 050051 is is the data card for volume V5, and card 050211 is the data card for volume V21. The underlined number on these cards is the volume flow area. This quantity was varied from 3.67 square feet for the area ratio (AR) = 1.0 case to 7.34 square feet for the AR = 0.5 case. The example shown in Table 5 is the AR = 0.7 case.

Table 6 is the input deck for RELAP4-SM used in the sensitivity study of Chapter Four. Note that the volume flow areas for V5 and V21 (cards 050051 and 050211) are 5.24 square feet, the optimum value found in Chapter Three. The only three cards changed in this deck to produce the different critical flow model runs were the title card (the first card in Table 6), and the junction data cards 080271 and 080281, for break junctions J27 and J28, respectively. The underlined quantities on these cards are the critical

flow model selection indices ICHOKE and JCHOKE. JCHOKE is the first underlined quantity, ICHOKE is the second. The values of JCHOKE and ICKOKE determine which critical flow model is to be used for that junction. Table V, page I-147 of the RELAP4 Users Manual is used to determine the values of JCHOKE and ICHOKE for the desired critical flow model. In the example shown, for junctions J27 and J28, the values are JCHOKE = 2, ICHOKE = 1 which indicate that the Sonic critical flow model is to be used for junctions J27 and J28. Note that all other junctions are set up to use the inertial flow model (ie. JCHOKE = -1, ICHOKE = 1).

TABLE 5. EVALUATION MODEL INPUT DATA DECK

```
-BWR EVALUATION MODEL 200% BREAK USING 7 X 7 FUEL
*234567890123456789012345678901234567890123456789012345678901234567890
*10001 LDM EDI NTS TRP VOL BUB TDV JUN PMP CKV NLK FLL SLBV GOM MAT COR
010001 -2   9   5  10  23  4 0 33 2 4 2 4 25 10 5 5 0 1
010002     3388.      1.0
010003   0   1   1   1
020000  AP 11 JW 27 JW 28 JW 29 JW 16 ML 4 SR 23 CR 23 TD 27
030010 1   100   5   0   .001   .00001    .1  2000.
030020 5    8    3   0    .01   .000001   1.
030030 20  10   2   0   .01     .000001   60.
030040 20  25   1   0    .01    .000001   130.
030050 20  25   1   0    .01    .00001    2000.
030003 50
040010 1  1   0   0  60.0  0.
040020 1 -4   3   0  40.0    0.
040030 2  1   0   0    0.0   0.
040040 3  1   0   0    0.001 0.
040050 4  1   0   0   .002   0.
040060 5  1   0   0   1.0    0.
040070 6  1   0   0   1.E6   0.
040080 7 -5   4   0   21.5  26.5
040090 8  1   0   0   .001   1.E6
040100 9 -5   4   0   21.38  120.
*5XXXX VOLUME DATA CARDS
050011 2 0 1039.    -1. .091632 1548.   22.25 22.25 0 224. 0.   29.92 0
050021 2 0 1028.28 -1. .002448 6703.   12.25  5.27 0 497. 0.   41.75 0
050031 1 0 1024.98 -1. .999     3777.   21.25 21.25 0 497. 0.   51.25 0
050041 3 0 1031.93 532.3 -1.    3177.   32.23 32.23 0 165. 0.   10.02 0
050051 0 0 1024.    532.3 -1.   125.25 26.    26.    0 5.24 0.   -14.   0
050061 0 0 1126.17 533.25 -1.   63.     3.     3.     0 4.0  0.   -14.   0
050071 0 0 1226.17 533.25 -1.   366.    40.53 40.53 0 3.2  0.   -14.   0
050081 0 0 1024.    512.30 -1.  136.    26.    26.    0 3.67 0.   -14.   0
050091 0 0 1126.17 533.25 -1.   63.     3.     3.     0 4.0  0.   -14.   0
050101 0 0 1226.17 533.25 -1.   366.    40.53 40.53 0 3.2  0.   -14.   0
050111 2 0 1062.16 532.53 -1.   2131.5 17.20 17.20 0 120. 0.    0.    23
050121 2 0 1054.67 549.337 -1. 223.   2.85 2.85 0 81.091 .0473 17.82 13
050131 2 0 1052.97 -1. .037157 223.   2.75 2.75 0 81.091 .0473 20.67 14
050141 2 0 1051.52 -1. .050567 81.09 1.    1.    0 81.091 .0473 23.42 15
050151 2 0 1049.87 -1. .091994 223.   2.75 2.75 0 81.091 .0473 24.42 16
050161 2 0 1047.65 -1. .139875 223.   2.75 2.75 0 81.091 .0473 27.17 1
050171 2 0 1054.28 532.53 -1.   942.47 18.12 18.12 0 52.301 0. 0.     18
050181 2 0 1045.86 532.67 -1. 534.53 12.35 12.35 0 43.635 0. 17.92   1
050191 0 0 1059.2   532.53 -1. 115.    15.7  15.7   0 19.69  0. 10.02  0
050201 0 0 1059.2   532.53 -1. 115.    15.7 15.7    0 19.69  0. 10.02  0
050211 0 0 1030.8   532.30 -1. 10.75  2.2    2.2    0 5.24   0. 10.     0
050221 4 0 14.7     100.   0.6  3.43E6 250.   0.0    0 1000. 100. -10.   0
050231 2 0 1055.48 532.53 -1. 20.5   1.25  1.25  0 81.09  0. 16.77  12
 *6000 LIQUID LEVEL CALCULATION CARD
060000 11 23 12 13 14 15 16 17 18 19 20 1
060001 0.0  0.0  0.0  0.0  0.0
*60002 WALLIS SLIP CORRELATION CARD
*60002 WALSC1 WALSC2
*6XXX1 BUBBLE DATA CARDS
*6XXX1 ALPH VBUB
060011 1.0  0.0
060021 0.0  3.0
060031 0.8  3.0
060041  0.  1.E6
*60001 SLIP VELOCITY CARD
*8XXXY JUNCTION DATA CARD
*23456789012345678901234567890123456789012345678901234567890123456789012
080011  1  2 0 0 29583. 191.1 52.17 0. 0. 0. 1 0 3 0 0.0 0. 11 0 1.0 0
080021  2  3 0 0 4074.3135 312. 52.25 0. 0. 0. 1 0 3 0 0.0 0. 11 0 0.0 0
080031  2  4 0 0 25444. 165.  42.0  0. 0. 0. 1 0 3 0 0.0 0. 11 0 0.0 0
080041 4 20 0 0 10041.5 3.112 25. 30. .2084 1.17 2 0 0 2 0.0 0. 11 0 0. 0
080051 4  21 0 0 4750.  3.67 11.0   0. 0. 0. 1 0 3 0 0.0 0. 11 0 0.0 0
080061 5  6 -1 0 4750.  3.67 -13.   0. 0. 0. 0 0 3 0 0.0 0. 11 0 0. 0
080071 6  7  1 0 4750.  3.2  -13.   0. 0. 0. 0 0 3 0 0.0 0. 11 0. 0. 0
080081 7 20  0 0 4750.  .538 25. 47. .2373 6.8 0 0 0 2 0. 0. 11 0 0. 0
080091 4 8   0 0 4750.  3.67 11.0   0. 0. 0. 1 0 3 0 0.0 0. 11 0 0. 0
080101 8  9 -2 0 4750.  3.67 -13.   0. 0. 0. 0 0 3 0 0.  0. 11 0 0. 0
080111 9  10 2 0 4750.  3.2  -13.   0. 0. 0. 0 0 3 0 0.  0. 11 0 0. 0
080121 10 19 0 0 4750.  .538 25. 47. .2373 6.8 0 0 0 2 0. 0. 11 0 0. 0
080131 4 19 0 0 10041.5 3.112 25. 30. .2084 1.17 2 0 0 2 0. 0. 11 0. 0. 0
080141 23 12 0 0 26639.  81.09  17.92 0. 0. 0. 0 0 3 0 0. 0. 11 0 1.0 0
080151 12 13 0 0 26639.  81.09  20.67 0. 0. 0. 0 0 3 0 0. 0. 11 0 1.0 0
080161 13 14 0 0 26639.  81.09  23.42 0. 0. 0. 0 0 3 0 0. 0. 11 0 1.0 0
```

TABLE 5. (cont.)

```
080171 14 15 0 0 26639.   81.09   24.42 0. 0. 0. 0 0 3 0 0. 0. 11 0 1.0 0
080181 15 16 0 0 26639.   81.09   27.17 0. 0. 0. 0 0 3 0 0. 0. 11 0 1.0 0
080191 16  1 0 0 26639.   37.13   29.92 0. 0. 0. 0 0 3 0 0. 0. 11 0 1.0 0
080201 11 17 0 0 2944.    2.246   17.0  0. 0. 0. 1 0 3 0 1.0 0. 11 0 0.0 0
080211 17 18 0 0 2944.    26.20   18.02 0. 0. 0. 0 0 3 0 0. 0. 11 0 0.0 0
080221 18  1 0 0 2944.    43.635  30.02 0. 0. 0. 0 0 3 0 0. 0. 11 0 1.0 0
080231 19 11 0 0 14791.5  19.69   10.12 0. 0. 0. 1 0 3 0 0. 0. 11 0 0.0 0
080241 20 11 0 0 14791.5  19.69   10.12 0. 0. 0. 1 0 3 0 0. 0. 11 0 0.0 0
080251 21 5  0 1 4750.    3.67    11.0  0. 0. 0. 0 0 3 0 0. 0. 11 0 0.0 0
080261 3 22  0 3 0.       .484    55.0  1. 1. 1. 0 0 0 0 0. 0. 11 0 0.0 0
080271 21 22 0 4 0.       3.67    11.   0. 1. .5 0 0 2 0 0. .9 11 0 0.0 0
080281 22 5  0 4 0.       3.67    11.   0. .5 1. 0 0 2 0 0. .9 11 0 0.0 0
080291 11 23 0 0 26639.  20.32    17.0  0. 0. 0. 1 0 3 0 0. 0. 11 0 1.0 0
080301 0 4   1 0 4074.3135 4.712  40.   0. 0. 0. 0 0 3 0 0. 0. 11 0 0.0 0
080311 0 3 2 2 -4074.3135 14.75   72.   0. 0. 0. 0 0 3 0 0. 0. 11 0 0.0 0
080321 0 1 3 0 0.         1.0     30.   0. 0. 0. 0 0 3 0 0. 0. 11 0 0.0 0
080331 0 10 4 0 0.        1.00    25.   1. 0. 0. 0 0 0 0 0. 0. 11 0 0.0 0
082000       1
*90XXY PUMP DESCRIPTION DATA CARDS
090011  3  4  0  1 0 1668.  1.0  44943.  710.3  22200.  20000.  47.17    0.  0
090021  3  4  0  1 0 1668.  1.0  44943.  710.3  22200.  20000.  47.17    0.  0
091001 -11 0.  0.   .1   0.   .15  .05  .24  .8   .3   .96  .4   .98  .6   .97
091002      .8  .9   .9   .8   .96  .5   1.0  0.
092001 -2 0. 0. 1. 0.
095011  0.  0.  0.
095021  0.  0.  0.
100000  0  0 16  0
103011  1  1  5 0.0   1.31   0.25   1.25   0.5   1.20   0.75   1.12   1.0   1.0
103021  1  2  5 0.0   -0.9   .25    -.5    .5    -.05   .75    .4     1.0   1.0
103031  1  3  5 -1.0  2.1    -.75   1.775  -0.5  1.54   -.25   1.4    0.    1.31
103041  1  4  5 -1.0  2.1    -.75   1.50   -0.5  1.13   -.25   .92    0.    .825
103051  1  5  5 0.    .4     .25    .53    .5    .625   .75    .80    1.0   1.0
103061  1  6  5 0.    .825   .25    .79    .5    .815   .75    .90    1.0   1.0
103071  1  7  5 -1.0  -1.8   -.75   -1.    -.5   -.4    -.25   .1     0.    .4
103081  1  8  5 -1.0  -1.8   -.75   -1.72  -.5   -1.54  -.25   -1.27  0.    -.9
103091  2  1  5 0.    .55    .25    .63    .5    .71    .75    .86    1.0   1.0
103101  2  2  5 0.    -.55   .2     -.175  .4    .0     .75    .58    1.0   1.0
103111  2  3  5 -1.0  1.77   -.75   1.23   -.5   .83    -.25   .62    0.    .55
103121  2  4  5 -1.0  1.77   -.75   1.52   -.5   1.32   -.25   1.13   0.    1.0
103131  2  5  5 0.    -.8    0.2    -.375  0.5   -.1    .75    .15    1.0   .43
103141  2  6  5 0.    1.0    .25    .88    .5    .75    .75    .61    1.0   .43
103151  2  7  5 -1.   -3.45  -.75   -2.75  -.50  -2.0   -.25   -1.375 0.    -.8
103161  2  8  5 -1.   -3.45  -.75   -2.62  -.50  -1.583 -.25   -1.15  0.    -.55
*11XXXO VALVE DATA CARDS
110010  4  0. 0 0.  0.  0.  0.
110020  5  2  0  0.  0.  0.  0.
110030 -9  0. 0  0.  0.  0.  0.
110040  -3  0. 0 0. 0. 0. 0.
*12XXYY  LEAK TABLE DATA CARDS
120101  -2  9  30.  0 1.  1000.  1.
120201  6 5 14.7 0. 1. 2.25 1. 2.5 .667 2.75 .333 3. 0. 10000. 0.
*13XXYY  FILL TABLE DATA DARDS
*3XX00 TRIP TYPE POINTS ICALC UNITS     PORT     HORX
130100   2   1      4       1   LBS/SEC  1050.    401.11324
130101  0. 864.6676 1. 864.6676 4.0 0. 10000. 0.
130200   2   2      4       3   LBS/SEC  548.     .999
130201  0. 0. 940. 0. 1025. -276.2246 3000. -276.2246
130300   7   2     11       3   GAL/MIN  212.    0.0
130301 0. 15150. 59. 14200. 137. 12500. 178. 11550. 237. 9470.
130302 268. 7576. 280. 5682. 287. 3788. 297. 1894. 304. 0. 10000. 0.
130400   7   2      9       3   GAL/MIN  212.      0.
130401 17.6 4355. 23.7 4309. 26.1 4291. 41.2 4175. 42.4 4166.
130402 98. 3708. 102. 3672. 310. 0. 3000. 0.
*14000 KINETICS CONSTANTS
*14000 PWR  MUL  BIL   REC   UDUF
140000  3    1   116.   0.    1.
*141001 SCRAM TABLE DATA CARDS
141001 -8  4 0. 0. 0.9 0. 1.075 -.4 1.6 -4. 2.7 -10. 5.7 -28.1 8. -30. 10. -30.
*142001 DENSITY REACTIVITY DATA CARDS
142001 -10  .2  -11.55  .3  -8.830  .4  -6.690  .5  -5.01  .6  -3.64  .7  -2.51
142002 .8  -1.55  .9  -0.73  1.  0.  1.1  0.
*143001 DOPPLER TABLE DATA CARDS
143001 -6  0. 1.85  1000. 0. 2000. -1.71 3000. -3. 4000. -4.28 5000. -5.43
```

TABLE 5. (cont.)

```
*140XX0 REACTIVITY COEFFICIENT DATA CARDS
140010  .148289  .148289  0. 0.
140020  .341782  .341782  0. 0.
140030  .019858  .019858  0. 0.
140040  .341782  .341782  0. 0.
140050  .148289  .148289  0. 0.
*15XXX HEAT SLAB DATA
150011 0  3  2 0 0 11 11 0.  687.  422.  0. 0. 0. 0. 0. 0.
150012 0. 0.
150021 0  2  2 0 0 11 11 0.  1368. 698.  0. 0. 0. 0. 0. 0.
150022 0. 0.
150031 0 4 2 0 0 11 11 0.    1916. 977.  0. 0. 0. 0. 0. 0.
150032 0. 0.
150041 0 11 2 0 0 11 11 0.   687.  385.  0. 0. 0. 0. 0. 0.
150042 0. 0.
150051 4 18 3 0 0 11 11 1355. 1355. 239. 0. 0. 0. 0. 0. 0.
150052 0. 0.
150061 1 2 4 0 0 11 11 2288.  2288. 286. 0. 0. 0. 0. 0. 0.
150062 0. 10.42
150071 11 23 5 0 0 11 11 197. 197.  65.  0. 0. 0. 0. 0. 0.
150072 0. 0.
150081 16 1 5 0 0 11 11 94. 94.     31.  0. 0. 0. 0. 0. 0.
150082 0. 0.
150091 11 17 6 0 0 11 11 6884. 6884. 95. 0. 0. 0. 0. 0. 0.
150092  0.  17.1
150101 0 11 7 0 0 11 11 0. 736. 46.      0. 0. 0. 0. 0. 0.
150102 0. 0.
150111 2 3 8 0 0 11 11 4380. 4380. 184.  0. 0. 0. 0. 0. 0.
150112 0. 0.
150121 0 5 9 0 0 11 11 0     450.   36.  0. 0. 0. 0. 0. 0.
150122 0. 0.
150131 0 8 9 0 0 11 11 0.    450.   36.  0. 0. 0. 0. 0. 0.
150132 0. 0.
150141 0 7 9 0 0 11 11 0.    838.   67.  0. 0. 0. 0. 0. 0.
150142 0. 0.
150151 0 10 9 0 0 11 11 0.   838.   67.  0. 0. 0. 0. 0. 0.
150152 0. 0.
150161 12 18 10 0 0 11 11 1096.8 1096.8 25.67 0. 0. 0. 0. 1.375 1.375
150162 0. 2.74
150171 13 18 10 1 0 11 11 1096.8 1096.8 25.67 0. 0. 0. 0. 4.125 4.125
150172 2.76 5.49
150181 14 18 10 1 0 11 11 398.84 398.84 9.334 0. 0. 0. 0. 6.0 6.0
150182 5.51 6.49
150191 15 18 10 1 0 11 11 1096.8 1096.8 25.67 0. 0. 0. 0. 7.875 7.875
150192 6.51 9.24
150201 16 18 10 1 0 11 11 1096.8 1096.8 25.67 0. 0. 0. 0. 10.625 10.625
150202 9.26 11.99
150211 0 12 1 0 0 11 11 0. 15175.52  178.039 0. .048 0. .0588 1.375 1.375
150212 0. 0.
150221 0 13 1 1 0 11 11 0. 15175.52  178.039 0. .048 0. .0588 4.125 4.125
150222 0. 0.
150231 0 14 1 1 0 11 11 0. 5518.372 64.741 0 .048 0. .0588 6.0 6.0
150232 0. 0.
150241 0 15 1 1 0 11 11 0. 15175.52 178.039 0. .048 0. .0588 7.875 7.875
150242 0. 0.
150251 0 16 1 1 0 11 11 0. 15175.52 178.039 0. .048 0. .0588 10.625 10.625
150252 0. 0.
*234567890123456789012345678901234567890123456789012345678901234567890
*16000 CORE SECTION DATA
*16000 SLB  NODE    CLAD    QFRAC
160010 21  7 9 15    0.    .17721
160020 22  7 9 15    0.    .26902
160030 23  7 9 15    0.    .10754
160040 24  7 9 15    0.    .26902
160050 25  7 9 15    0.    .17721
160015  0  0  96.07 .8    .6   .965   .95 0 0 .05 0 0 0 .08333 .9714  .01988 0 0
160025  0  0 0.     .8    .6   .965   .95 0 0 .05 0 0 0 .08333 0.     .01988 0 0
160035  0  0 0.     .8    .6   .965   .95 0 0 .05 0 0 0 .08333 0.     .01988 0 0
160045  0  0 0.     .8    .6   .965   .95 0 0 .05 0 0 0 .08333 0.     .01988 0 0
160055  0  0  .1259 .8    .6   .965   .95 0 0 .05 0 0 0 .08333 .00127 .01988 0 0
```

TABLE 5. (cont.)

```
*17XXYY SLAB GEOMETRY DATA CARDS
170101  2  3  1  6 0.0      .020071 1.0
170102  1     2  2          .000721 0.
170103  0     3  8          .00267  0.
170201  1  2  4  3 0.0      .4      0.
170202  0     5  1          .0208   0.
170301  1  1  5  1 0.       .17     0.
170401  1  1  5  1 0.       .125    0.
170501  1  1  5  1 0.       .33     0.
170601  1  1  5  1 0.       .0138   0.
170701  1  1  5  1 0.       .0625   0.
170801  1  1  5  1 0.       .042    0.
170901  1  1  5  1 0.       .08     0.
171001  1  1  5  1 0.       .0234   0.
180100 -20  500.   3.341  650.   2.971  800.   2.677  950.   2.439  1100.  2.242
180101       1250.  2.078  1400.  1.940  1550.  1.823  1700.  1.724  1850.  1.639
180102       2000.  1.568  2150.  1.507  2300.  1.457  2450.  1.415  2600.  1.382
180103       3100.  1.323  3600.  1.333  4100.  1.406  4600.  1.538  5100.  1.730
180200    2           32.       .41562    5400.      .41562
180300   18           32.       7.812     212.       7.992     392.       8.208
180301                572.      8.784     752.       9.540     932.       10.404
180302                1112.     11.268    1292.      12.492    1472.      13.176
180303                1652.     13.968    1832.      14.796    2012.      16.128
180304                2192.     17.784    2372.      19.656    2552.      21.780
180305                2732.     24.048    3092.      28.908    3360.      33.120
180401 -5  32. 30. 212. 29.5 392. 28.3 572. 26.6 752. 24.7
180501 -2  200. 8.33 1200. 12.92
190100   16                32. 34.45          122. 38.35          212. 40.95
190101                    392. 43.55          752. 46.8          2012. 51.35
190102                   2732. 52.65      3092. 56.55  3452. 63.05
190103                   3812. 72.8          4352. 89.7          4532. 94.25
190104                   4712. 98.15         4892. 100.1         5144. 101.4
190105                   8000. 101.4
190200    2           32.       .000075   5400.      .000075
190300   5   0.0   28.392
190301   1480.3   34.476   1675.0   85.176
190302   1787.5   34.476   3500.0   34.476
190401 -7 130. 56.9 350. 60.8 450. 62.3 530. 65.2 620. 67.2 710. 70.2 800. 77.5
190501 -10 68. 52.8 200. 56.7 400. 61.6 600. 64. 800. 66. 1000. .67
190502      1200. 68.4 1400. 71.8 1600. 75.8 1800. 80.6
200101 -2 0. 3.718E-6  5000.  1.2653E-5
200201 -2 0. 0. 5000. 0.
200301  -4  0.  3.094E-6  1652.  4.706E-6  1653.  5.389E-6  5000. 5.389E-6
200401 -2  0.  0. 5000. 0.
200501 -2  0.  0. 5000. 0.
250001 1 2 3 0 .0615
260001 1 2 3 4 6 6 6 6 11 1E7 11 0 0 0 0 0 0 0 0 0
270001 -14 2500. 0. 2200. 98.7 1620. 197. 1730. 395. 1660. 592. 1600. 790.
270002 1540. 987. 1480. 1184. 1440. 1382. 1400. 1579. 1370. 1777. 1335. 1974.
270003  1310. 2172. 1280. 2369.
280001 -4  34.  0.  34.  150.  21.  200.  21.  1000.
290001 -14 2500. 0. 2200. 98.7 1620. 197. 1730. 395. 1660. 592. 1600. 790.
290002 1540. 987. 1480. 1184. 1440. 1382. 1400. 1579. 1370. 1777. 1335. 1974.
290003  1310. 2172. 1280. 2369.
300001 -14 131. 0. 131. 98.7 62. 197. 47. 395. 69. 592. 95. 790. 116. 987.
300002   131. 1184. 137. 1382. 131. 1579. 121. 1777. 100. 1974. 76. 2172.
300003  58. 2369.
.
```

TABLE 6. STANDARD MODEL INPUT DATA DECK

```
=BWR BEST ESTIMATE 200%BRK CRITICAL FLOW - SONIC
*234567890123456789012345678901234567890123456789012345678901234567890
*10001 LDM EDI NTS TRP VOL BUB TDV JUN PMP CKV NLK FLL SLBV GOM MAT COR
010001 -2    9    5   10   23   4 0 33 2 4 2 4 25 10 5 5 0 0
010002     3388.       1.0
020000  AP 11 JW 27 JW 28 JW 29 JW 16 ML 4 SR 23 CR 23 TD 27
030010 1    100    5    0    .001    .00001     .1  2000.
030020 5      8    3    0     .01    .000001    1.
030030 20   10    2    0    .01     .000001    60.
030040 20   25    1    0     .01    .000001    130.
030050 20   25    1    0     .01    .00001     2000.
030003 50
040010 1   1    0    0    60.0    0.
040020 1  -4    3    0   40.0     0.
040030 2   1    0    0     0.0    0.
040040 3   1    0    0     0.001  0.
040050 4   1    0    0    .002    0.
040060 5   1    0    0    1.0     0.
040070 6   1    0    0    1.E6    0.
040080 7  -5    4    0    21.5   26.5
040090 8   1    0    0    .001    1.E6
040100 9  -5    4    0    21.38  120.
*5XXXX VOLUME DATA CARDS
050011 2 0 1039.    -1. .091632 1548.   22.25 22.25 0 224. 0.   29.92 0
050021 2 0 1028.28 -1. .002448 6703.   12.25  5.27 0 497. 0.   41.75 0
050031 1 0 1024.98 -1. .999     3777.   21.25 21.25 0 497. 0.   51.25 0
050041 3 0 1031.93 532.3 -1.    3177.   32.23 32.23 0 165. 0.   10.02 0
050051 0 0 1024.    532.3 -1.   125.25 26.    26.    0 5.24 0.  -14.   0
050061 0 0 1126.17 533.25 -1.   63.     3.     3.     0 4.0  0.  -14.   0
050071 0 0 1226.17 533.25 -1.   366.    40.53 40.53 0 3.2  0.  -14.   0
050081 0 0 1024.    532.30 -1.  136.    26.    26.    0 3.67 0.  -14.   0
050091 0 0 1126.17 533.25 -1.   63.     3.     3.     0 4.0  0.  -14.   0
050101 0 0 1226.17 533.25 -1.   366.    40.53 40.53 0 3.2  0.  -14.   0
050111 2 0 1062.16 532.53 -1.   2131.5 17.20 17.20 0 120. 0.    0.    23
050121 2 0 1054.67 549.337 -1. 223.   2.85 2.85 0 81.091 .0473 17.82 13
050131 2 0 1052.97 -1. .037157 223.   2.75 2.75 0 81.091 .0473 20.67 14
050141 2 0 1051.52 -1. .050567 81.09 1.    1.    0 81.091 .0473 23.42 15
050151 2 0 1049.87 -1. .091994 223.   2.75 2.75 0 81.091 .0473 24.42 16
050161 2 0 1047.65 -1. .139875 223.   2.75 2.75 0 81.091 .0473 27.17 1
050171 2 0 1054.28 532.53 -1.   942.47 18.12 18.12 0 52.301 0. 0.     18
050181 2 0 1045.86 532.67 -1. 534.53 12.35 12.35 0 43.635 0. 17.92  1
050191 0 0 1059.2   532.53 -1. 115.    15.7  15.7  0 19.69  0. 10.02  0
050201 0 0 1059.2   532.53 -1. 115.    15.7 15.7   0 19.69  0. 10.02  0
050211 0 0 1030.8   532.30 -1. 10.75   2.2   2.2   0 5.24   0. 10.    0
050221 4 0 14.7     100.  0.6  3.43E6 250.   0.0   1 1000. 100. -10.  0
050231 2 0 1055.48 532.53 -1. 20.5    1.25  1.25  0 81.09  0. 16.77  12
 *6000 LIQUID LEVEL CALCULATION CARD
060000 11 23 12 13 14 15 16 17 18 19 20 1
060001 0.0  0.0  0.0  0.0  0.0
*60002 WALLIS SLIP CORRELATION CARD
*60002 WALSC1 WALSC2
*6XXX1 BUBBLE DATA CARDS
*6XXX1 ALPH VBUB
060011 1.0  0.0
060021 0.0  3.0
060031 0.8  3.0
060041  0.  1.E6
*60001 SLIP VELOCITY CARD
*8XXXY JUNCTION DATA CARD
*234567890123456789012345678901234567890123456789012345678901234567890123456789012
080011  1  2 0 0 29583. 191.1 52.17 0. 0. 0. 1 -1 3 0 0.0 0. 1 0 1.0 0
080021  2  3 0 0 4074.3135 312. 52.25 0. 0. 0. 1 -1 3 0 0.0 0. 1 0 0.0 0
080031  2  4 0 0 25444. 165.  42.0  0. 0. 0. 1 -1 3 0 0.0 0. 1 0 0.0 0
080041 4 20 0 0 10041.5 3.112 25. 30. .2084 1.17 2 -1 0 2 0.0 0. 1 0 0. 0
080051 4  21 0 0 4750.  3.67 11.0   0. 0. 0. 1 -1 3 0 0.0 0. 1 0 0.0 0
080061 5  6 -1 0 4750.  3.67 -13.   0. 0. 0. 0 -1 3 0 0.0 0. 1 0 0.0 0
080071 6  7  1 0 4750.  3.2  -13.   0. 0. 0. 0 -1 3 0 0.0 0. 1 0 0.0 0
080081 7 20  0 0 4750.  .538 25. 47. .2373 6.8 0 -1 0 2 0. 0. 1 0 0.0 0
080091 4 8   0 0 4750.  3.67 11.0   0. 0. 0. 1 -1 3 0 0.0 0. 1 0 0.0 0
080101 8  9 -2 0 4750.  3.67 -13.   0. 0. 0. 0 -1 3 0 0.  0. 1 0 0.0 0
080111 9  10 2 0 4750.  3.2  -13.   0. 0. 0. 0 -1 3 0 0.  0. 1 0 0.0 0
080121 10 19 0 0 4750.  .538 25. 47. .2373 6.8 0 -1 0 2 0. 0. 1 0 0.0 0
080131 4 19 0 0 10041.5 3.112 25. 30. .2084 1.17 2 -1 0 2 0. 0. 1 0 0. 0
080141 23 12 0 0 26639.  81.09  17.92 0. 0. 0. 0 -1 3 0 0. 0. 1 0 1.0 0
080151 12 13 0 0 26639.  81.09  20.67 0. 0. 0. 0 -1 3 0 0. 0. 1 0 1.0 0
080161 13 14 0 0 26639.  81.09  23.42 0. 0. 0. 0 -1 3 0 0. 0. 1 0 1.0 0
```

TABLE 6. (cont.)

```
080171 14 15 0 0 26639.   81.09   24.42 0. 0. 0. 0 -1 3 0 0. 0. 1 0 1.0 0
080181 15 16 0 0 26639.   81.09   27.17 0. 0. 0. 0 -1 3 0 0. 0. 1 0 1.0 0
080191 16  1 0 0 26639.   37.13   29.92 0. 0. 0. 0 -1 3 0 0. 0. 1 0 1.0 0
080201 11 17 0 0 2944.    2.246  17.0  0. 0. 0. 1 -1 3 0 1.0 0. 1 0 0.0 0
080211 17 18 0 0 2944.    26.20  18.02 0. 0. 0. 0 -1 3 0 0. 0. 1 0 0.0 0
080221 18  1 0 0 2944.    43.635 30.02 0. 0. 0. 0 -1 3 0 0. 0. 1 0 1.0 0
080231 19 11 0 0 14791.5  19.69  10.12 0. 0. 0. 1 -1 3 0 0. 0. 1 0 0.0 0
080241 20 11 0 0 14791.5  19.69  10.12 0. 0. 0. 1 -1 3 0 0. 0. 1 0 0.0 0
080251 21 5  0 1 4750.    3.67   11.0  0. 0. 0. 0 -1 3 0 0. 0. 1 0 0.0 0
080261 3 22  0 3 0.       .484   55.0  1. 1. 1. 0 -1 0 0 0. 0. 1 0 0.0 0
080271 21 22 0 4 0.       3.67   11.   0. 1. .5 0 2 2 0 0. .9 1 0 0.0 0
080281 22 5  0 4 0.       3.67   11.   0. .5 1. 0 2 2 0 0. .9 1 0 0.0 0
080291 11 23 0 0 26639.  20.32   17.0  0. 0. 0. 1 -1 3 0 0. 0. 1 0 1.0 0
080301 0 4   1 0 4074.3135 4.712 40.   0. 0. 0. 0 -1 3 0 0. 0. 1 0 0.0 0
080311 0 3 2 2 -4074.3135 14.75  72.   0. 0. 0. 0 -1 3 0 0. 0. 1 0 0.0 0
080321 0 1 3 0 0.         1.0    30.   0. 0. 0. 0 -1 3 0 0. 0. 1 0 0.0 0
080331 0 10 4 0 0.        1.00   25.   1. 0. 0. 0 -1 0 0 0. 0. 1 0 0.0 0
*90XXY PUMP DESCRIPTION DATA CARDS
090011  3  4  0  1 0 1668.  1.0  44943.  710.3  22200.  20000.  47.17    0.  0
090021  3  4  0  1 0 1668.  1.0  44943.  710.3  22200.  20000.  47.17    0.  0
091001 -11 0.  0.   .1   0.   .15  .05  .24  .8   .3   .96  .4   .98  .6   .97
091002     .8  .9   .9   .8   .96  .5   1.0  0.
092001 -2 0. 0. 1. 0.
095011  0.  0.  0.
095021  0.  0.  0.
100000  0  0 16  0
103011  1  1  5 0.0   1.31   0.25   1.25   0.5   1.20   0.75   1.12   1.0   1.0
103021  1  2  5 0.0   -0.9   .25    -.5    .5    -.05   .75    .4     1.0   1.0
103031  1  3  5 -1.0  2.1    -.75   1.775  -0.5  1.54   -.25   1.4    0.    1.31
103041  1  4  5 -1.0  2.1    -.75   1.50   -0.5  1.13   -.25   .92    0.    .825
103051  1  5  5 0.    .4     .25    .53    .5    .625   .75    .80    1.0   1.0
103061  1  6  5 0.    .825   .25    .79    .5    .815   .75    .90    1.0   1.0
103071  1  7  5 -1.0  -1.8   -.75   -1.    -.5   -.4    -.25   .1     0.    .4
103081  1  8  5 -1.0  -1.8   -.75   -1.72  -.5   -1.54  -.25   -1.27  0.    -.9
103091  2  1  5 0.    .55    .25    .63    .5    .71    .75    .86    1.0   1.0
103101  2  2  5 0.    -.55   .2     -.175  .4    .0     .75    .58    1.0   1.0
103111  2  3  5 -1.0  1.77   -.75   1.23   -.5   .83    -.25   .62    0.    .55
103121  2  4  5 -1.0  1.77   -.75   1.52   -.5   1.32   -.25   1.13   0.    1.0
103131  2  5  5 0.    -.8    0.2    -.375  0.5   -.1    .75    .15    1.0   .43
103141  2  6  5 0.    1.0    .25    .88    .5    .75    .75    .61    1.0   .43
103151  2  7  5 -1.   -3.45  -.75   -2.75  -.50  -2.0   -.25   -1.375 0.    -.8
103161  2  8  5 -1.   -3.45  -.75   -2.62  -.50  -1.583 -.25   -1.15  0.    -.55
*11XXXO VALVE DATA CARDS
110010  4  0. 0 0.  0.  0.  0.
110020  5  2  0  0.  0.  0.  0.
110030 -9  0. 0  0.  0.  0.  0.
110040  -3  0. 0 0. 0. 0. 0.
*12XXYY  LEAK TABLE DATA CARDS
120101  -2  9  30.  0 1.  1000.  1.
120201  6 5 14.7 0. 1. 2.25 1. 2.5 .667 2.75 .333 3. 0. 10000. 0.
*13XXYY  FILL TABLE DATA DARDS
*3XX00 TRIP TYPE POINTS ICALC UNITS     PORT     HORX
130100   2   1      4       1   LBS/SEC  1050.    401.11324
130101  0. 864.6676 1. 864.6676 4.0 0. 10000. 0.
130200   2   2      4       3   LBS/SEC  548.     .999
130201  0. 0. 940. 0. 1025. -276.2246 3000. -276.2246
130300   7   2     11       3   GAL/MIN  212.    0.0
130301 0. 15150. 59. 14200. 137. 12500. 178. 11550. 237. 9470.
130302 268. 7576. 280. 5682. 287. 3788. 297. 1894. 304. 0. 10000. 0.
130400   7   2      9       3   GAL/MIN  212.       0.
130401 17.6 4355. 23.7 4309. 26.1 4291. 41.2 4175. 42.4 4166.
130402 98. 3708. 102. 3672. 310. 0. 3000. 0.
*14000 KINETICS CONSTANTS
*14000 PWR  MUL  BIL   REC   UDUF
140000  3    0   116.   0.    1.
*141001 SCRAM TABLE DATA CARDS
141001 -8  4 0. 0. 0.9 0. 1.075 -.4 1.6 -4. 2.7 -10. 5.7 -28.1 8. -30. 10. -30.
*142001 DENSITY REACTIVITY DATA CARDS
142001 -10  .2  -11.55  .3  -8.830  .4  -6.690  .5  -5.01  .6  -3.64  .7  -2.51
142002 .8  -1.55  .9  -0.73  1.  0.  1.1  0.
*143001 DOPPLER TABLE DATA CARDS
143001 -6  0. 1.85  1000. 0. 2000. -1.71 3000. -3. 4000. -4.28 5000. -5.43
```

TABLE 6. (cont.)

```
*140XX0 REACTIVITY COEFFICIENT DATA CARDS
140010  .148289  .148289  0. 0.
140020  .341782  .341782  0. 0.
140030  .019858  .019858  0. 0.
140040  .341782  .341782  0. 0.
140050  .148289  .148289  0. 0.
*15XXX HEAT SLAB DATA
150011 0  3  2 0 0 0 0 0.  687.  422.  0. 0. 0. 0. 0. 0.
150012 0. 0.
150021 0  2  2 0 0 0 0 0.  1368. 698.  0. 0. 0. 0. 0. 0.
150022 0. 0.
150031 0 4 2 0 0 0 0 0.    1916. 977.  0. 0. 0. 0. 0. 0.
150032 0. 0.
150041 0 11 2 0 0 0 0 0.   687.  385.  0. 0. 0. 0. 0. 0.
150042 0. 0.
150051 4 18 3 0 0 0 0 1355. 1355. 239. 0. 0. 0. 0. 0. 0.
150052 0. 0.
150061 1 2 4 0 0 0 0 2288.  2288. 286. 0. 0. 0. 0. 0. 0.
150062 0. 10.42
150071 11 23 5 0 0 0 0 197. 197.  65.  0. 0. 0. 0. 0. 0.
150072 0. 0.
150081 16 1 5 0 0 0 0 94. 94.     31.  0. 0. 0. 0. 0. 0.
150082 0. 0.
150091 11 17 6 0 0 0 0 6884. 6884. 95. 0. 0. 0. 0. 0. 0.
150092  0.  17.1
150101 0 11 7 0 0 0 0 0. 736. 46.      0. 0. 0. 0. 0. 0.
150102 0. 0.
150111 2 3 8 0 0 0 0 4380. 4380. 184.  0. 0. 0. 0. 0. 0.
150112 0. 0.
150121 0 5 9 0 0 0 0 0     450.   36.  0. 0. 0. 0. 0. 0.
150122 0. 0.
150131 0 8 9 0 0 0 0 0.    450.   36.  0. 0. 0. 0. 0. 0.
150132 0. 0.
150141 0 7 9 0 0 0 0 0.    838.   67.  0. 0. 0. 0. 0. 0.
150142 0. 0.
150151 0 10 9 0 0 0 0 0.   838.   67.  0. 0. 0. 0. 0. 0.
150152 0. 0.
150161 12 18 10 0 0 0 0 1096.8 1096.8 25.67 0. 0. 0. 0. 1.375 1.375
150162 0. 2.74
150171 13 18 10 1 0 0 0 1096.8 1096.8 25.67 0. 0. 0. 0. 4.125 4.125
150172 2.76 5.49
150181 14 18 10 1 0 0 0 398.84 398.84 9.334 0. 0. 0. 0. 6.0 6.0
150182 5.51 6.49
150191 15 18 10 1 0 0 0 1096.8 1096.8 25.67 0. 0. 0. 0. 7.875 7.875
150192 6.51 9.24
150201 16 18 10 1 0 0 0 1096.8 1096.8 25.67 0. 0. 0. 0. 10.625 10.625
150202 9.26 11.99
150211 0 12 1 0 0 0 0 0. 15175.52  178.039 0. .048 0. .0588 1.375 1.375
150212 0. 0.
150221 0 13 1 1 0 0 0 0. 15175.52  178.039 0. .048 0. .0588 4.125 4.125
150222 0. 0.
150231 0 14 1 1 0 0 0 0. 5518.372 64.741 0 .048 0. .0588 6.0 6.0
150232 0. 0.
150241 0 15 1 1 0 0 0 0. 15175.52 178.039 0. .048 0. .0588 7.875 7.875
150242 0. 0.
150251 0 16 1 1 0 0 0 0. 15175.52 178.039 0. .048 0. .0588 10.625 10.625
150252 0. 0.
*234567890123456789012345678901234567890123456789012345678901234567890
*16000 CORE SECTION DATA
*16000 SLB  NODE     CLAD     OFRAC
160010 21   7 9 15     0.     .17721
160020 22   7 9 15     0.     .26902
160030 23   7 9 15     0.     .10754
160040 24   7 9 15     0.     .26902
160050 25   7 9 15     0.     .17721
```

TABLE 6. (cont.)

```
*17XXYY SLAB GEOMETRY DATA CARDS
170101   2   3   1   6 0.0       .020071 1.0
170102   1       2   2           .000721 0.
170103   0       3   8           .00267  0.
170201   1   2   4   3 0.0       .4      0.
170202   0       5   1           .0208   0.
170301   1   1   5   1 0.        .17     0.
170401   1   1   5   1 0.        .125    0.
170501   1   1   5   1 0.        .33     0.
170601   1   1   5   1 0.        .0138   0.
170701   1   1   5   1 0.        .0625   0.
170801   1   1   5   1 0.        .042    0.
170901   1   1   5   1 0.        .08     0.
171001   1   1   5   1 0.        .0234   0.
180100 -20   500.    3.341   650.    2.971   800.    2.677   950.    2.439   1100.   2.242
180101       1250.   2.078   1400.   1.940   1550.   1.823   1700.   1.724   1850.   1.639
180102       2000.   1.568   2150.   1.507   2300.   1.457   2450.   1.415   2600.   1.382
180103       3100.   1.323   3600.   1.333   4100.   1.406   4600.   1.538   5100.   1.730
180200     2             32.         .41562      5400.       .41562
180300    18             32.         7.812       212.        7.992       392.        8.208
180301                   572.        8.784       752.        9.540       932.        10.404
180302                   1112.       11.268      1292.       12.492      1472.       13.176
180303                   1652.       13.968      1832.       14.796      2012.       16.128
180304                   2192.       17.784      2372.       19.656      2552.       21.780
180305                   2732.       24.048      3092.       28.908      3360.       33.120
180401 -5   32. 30. 212. 29.5 392. 28.3 572. 26.6 752. 24.7
180501 -2   200. 8.33 1200. 12.92
190100    16                  32. 34.45           122. 38.35           212. 40.95
190101                      392. 43.55           752. 46.8           2012. 51.35
190102                     2732. 52.65      3092. 56.55  3452. 63.05
190103                     3812. 72.8           4352. 89.7           4532. 94.25
190104                     4712. 98.15          4892. 100.1          5144. 101.4
190105                     8000. 101.4
190200     2             32.         .000075     5400.       .000075
190300    5    0.0    28.392
190301    1480.3    34.476    1675.0    85.176
190302    1787.5    34.476    3500.0    34.476
190401 -7 130. 56.9 350. 60.8 450. 62.3 530. 65.2 620. 67.2 710. 70.2 800. 77.5
190501 -10 68. 52.8 200. 56.7 400. 61.6 600. 64. 800. 66. 1000. .67
190502      1200. 68.4 1400. 71.8 1600. 75.8 1800. 80.6
200101 -2 0. 3.718E-6   5000.   1.2653E-5
200201 -2 0. 0. 5000. 0.
200301  -4   0.   3.094E-6   1652.   4.706E-6   1653.   5.389E-6   5000. 5.389E-6
200401 -2   0.   0. 5000. 0.
200501 -2   0.   0. 5000. 0.
.
```

APPENDIX B

PLOT/RESTART DATA RETRIEVAL PROGRAM

This appendix describes a Fortran IV program written to extract data from the RELAP4 Plot/Restart tape. During RELAP4 problem execution there are two types of information written to the Plot/Restart tape. They are called common block records, and plot records. Common block records contain information required to restart the problem. Plot records contain data that may be useful for graphical display of the transient parameters of interest.

A plot record is written to the tape at time intervals specified by the user (ie. each time a minor edit is printed, a plot record is written to the Plot/Restart tape). The length of a plot record depends of the system being modeled and can be calculated as follows,

$$LEN = 21 + 20 + 24(NVOL) + 16(NJUN) + 20(NSLB)$$

where,

LEN = length of plot record in computer words,
NVOL = number of volumes in the RELAP4 model,
NJUN = number of junctions in the RELAP4 model,
NSLB = number of heat slabs in the RELAP4 model.

For the problem used in this study (ie. Hope Creek) NVOL = 23, NJUN = 33, NSLB = 25, and the the plot record length (LEN) is thus 1621 computer words. A computer word is four bytes or 32 alpha-numeric characters. Future reference to word will imply computer word, unless otherwise indicated.

The following is an explanation of the reason for the numbers used in the above equation; The first word of each plot record contains the letters 'PLOT'. The next twenty words of the plot record contain the problem title and the number of junctions and volumes in the system. The next twenty words are twenty system parameters, such as normalized power, total energy stored in the fuel, transient time, etc. (These parameters are listed on page II-228 of the RELAP4 Users Manual). The next 24 X NVOL words (in this case 552 words) contain the 24 volume parameters listed on page II-229 of the Users Manual. This information is written to the tape as follows. Words 1-23 are the average pressures in volumes 1-23, words 24-46 are the total mass in volumes 1-23, etc. The next 16 X NJUN words (in this case 528 words) contain the 16 junction parameters listed on page II-230 of the Users Manual. This information is written in the same order as the volume information (ie. words 1-33 are the mass flow rates for junctions 1-33, etc). The next 20 X NSLB words (500 words in this case) contain the twenty heat slab parameters listed on pages II-230 and II-231 of the

Users Manual. These parameters are written in the same order as the volume and junction data.

Table 7 is a listing of the program written to extract plotting data from the Plot/Restart tape. The numbers in the left column are sequence numbers used in the following program description. The program utilizes a Penn State library subroutine called PRECL/FBUF (21).

The name of the Plot/Restart tape from which data is to be extracted must be entered on lines 55 and 1250 (in the example shown the tape name is EDIT2). The data set name (DSN) on line 1250 must be the same as the as the DSN used to write information to the tape during problem execution (in the example DSN=TPOUT).

The first step of the program (line 400) is the CALL PRECL statement. This statement loads the entire first record from the Plot/Restart tape into a logical array called REC. The length of the record is also returned as the variable called LEN. A DO loop is then entered (line 450) where the following steps are taken. Line 500 checks the first four characters of the array REC. If the characters are not the letters 'PLOT' then the record is not a plot record, and execution skips to line 650, which is the CALL FBUF statement. This statement loads the next record of the tape into the array REC and execution returns to line 450. This process is continued until a plot record is found by line 500.

TABLE 7. PLOT/RESTART TAPE DATA RETRIEVAL PROGRAM

```
00050 /*USERID MVC01
00055 /*TAPE EDIT2
00100 // EXEC FGCG
00150 //SYSIN DD *
00200       LOGICAL*1 CNE
00250       INTEGER*2 LEN
00300       LOGICAL*1 REC(32000)
00350       NREC=1
00400       CALL PRECL('IN      ',LEN,NREC,REC)
00450       DO 1 I=1,9999999
00500       IF(CNE(REC,'PLOT',4))GO TO 1
00550       KLEN=LEN/4
00600       CALL OUT(REC,KLEN)
00650     1 CALL FBUF(&99,&88)
00700    99 STOP
00750    88 STOP
00800       END
00850       SUBROUTINE OUT(REC,KLEN)
00900       REAL REC(KLEN)
00950       WRITE(17,10)REC(39),REC(52),REC(620),REC(621),REC(622),
01000      $REC(229),REC(1169),REC(1219)
01005       WRITE(6,10)REC(39),REC(52),REC(620),REC(621),REC(622),
01010      $REC(229),REC(1169),REC(1219)
01050    10 FORMAT(F8.3,1P7E10.3)
01100       RETURN
01150       END
01200 //DATA.FT17F001 DD UNIT=BAT,FILES=$DEM6
01250 //DATA.IN DD UNIT=2400,VOL=SER=EDIT2,DSN=TPOUT
01300
```

When a plot record is found program execution goes to line 550 which divides the record length LEN by four, converting the record length from computer words to alpha-numeric words. The subroutine OUT is then called (line 600) and execution skips to line 850. Line 900 changes the array REC from a logical array to a real number array. Lines 950 and 1000 write the desired parameters (discussed below) to Fortran Unit 17, defined in line 1200 as a BAT file called, in this case $DEM6. Lines 1005 and 1010 write the same parameters to Fortran Unit 6, a line printer. Following printing of the desired parameters, program execution is returned to the main program at line 650. The program continues to process records until an end-of-file is encountered, when execution is stopped.

To determine the word number of the desired parameter to be printed, the following steps are taken;

For system parameters, the word number is simply 21 plus the number of the systen parameter. For example, the transient time is parameter number 18 (recall that parameter numbers are taken from the RELAP4 Users Manual on the pages noted earlier). Thus the word number for transient time is 21 + 18 = 39 and REC(39) contains this parameter.

For volume parameters, the word number is calculated as follows,

$$WN = 41 + (VPN - 1)NVOL + VOLN$$

where the new symbols are,

WN = word number of desired parameter

VPN = volume parameter number

VOLN = volume number of desired parameter.

For example, if the desired parameter is mixture level in volume 4, the word number is calculated as follows; The VPN for mixture level is 9. NVOL = 23, and VOLN = 4. Thus WN = 229, and REC(229) is the mixture level in volume 4.

For junction parameters the word number is calculated from,

$$WN = 41 + 24(NVOL) + (JPN - 1)NJUN + JUNN$$

where the new symbols are,

JPN = junction parameter number

JUNN = junction number of desired parameter.

For example, if the desired parameter is the flow rate in junction 27, the word number is calculated as follows; The JPN for flow rate is 1, NVOL = 23, NJUN = 33, and JUNN = 27. Thus WN = 620 and REC(620) is the flow rate at junction 27.

For heat slab parameters the word number is calculated from,

$$WN = 41 + 24(NVOL) + 16(NJUN) + (SLBPN - 1)NSLB + SLBN$$

where,

SLBPN = heat slab parameter number

SLBN = heat slab number.

For example, if the desired parameter is surface temperature, heat slab S23, the word number is calculated as follows; The SLBPN for surface temperature is 2, NVOL = 23, NJUN = 33, NSLB = 25, and SLBN = 23. Thus WN = 1169, and REC(1169) is the surface temperature of heat slab 23.

The central processing unit (CPU) time required for execution of the program depends on the amount of data to be processed. As a benchmark, processing of 400 records takes about fifty CPU seconds.

Thesis
C2214
c.1

Carle

A sensitivity study of the critical flow models used in RELAP4/ MOD5 blowdown analysis of a general electric BWR.

184676